Biogeosciences Discuss., doi:10.5194/bg-2017-154, 2017
Manuscript under review for journal Biogeosciences
Discussion started: 15 May 2017
© Author(s) 2017. CC-BY 3.0 License.

Biogeosciences Discussions
Open Access
EGU

$\delta^{11}B$ as monitor of calcification site pH in marine calcifying organisms

Jill N. Sutton[1], Yi-Wei Liu[1], Justin B. Ries[2], Maxence Guillermic[1], Emmanuel Ponzevera[3], and Robert A. Eagle [1,4,5]

[1]Université de Brest, UBO, CNRS, IRD, Ifremer, Institut Universitaire Européen de la Mer, LEMAR, Rue Dumont d'Urville, 29280, Plouzané, France
[2]Department of Marine and Environmental Sciences, Marine Science Center, Northeastern University, 430 Nahant Rd, Nahant, MA 01908, USA
[3]Unité de Recherche Géosciences Marines, Ifremer, 29280, Plouzané, France
[4]Institute of the Environment and Sustainability, University of California, Los Angeles, LaKretz Hall, 619 Charles E Young Dr E #300, Los Angeles, CA 90024, USA
[5]Atmospheric and Oceanic Sciences Department, University of California – Los Angeles, Maths Science Building, 520 Portola Plaza, Los Angeles, CA 90095, USA

Correspondence to: Jill-Naomi.Sutton@univ-brest.fr and robeagle@g.ucla.edu

Abstract. The isotope composition of boron (B) in marine biogenic carbonates has been predominantly studied as a proxy for monitoring past changes in seawater pH and carbonate chemistry. In order to derive seawater pH from boron isotope ratio data, a number of assumptions related to chemical kinetics and themodynamic isotope exchange reactions are necessary. Furthermore, the boron isotope composition ($\delta^{11}B$) of biogenic carbonates ($\delta^{11}B_{CaCO3}$) is assumed to reflect the $\delta^{11}B$ of dissolved borate ($B(OH)_4^-$) in seawater. Here we report the development of methodology for measuring the $\delta^{11}B$ in biogenic carbonate samples at the multi-collector inductively coupled mass spectrometry facility at Ifremer (Plouzané, France) and the evaluation of $\delta^{11}B_{CaCO3}$ in a diverse range of marine calcifying organisms. We evaluated the $\delta^{11}B_{CaCO3}$ of 6 species of marine calcifiers (a temperate coral, *Oculina arbuscula*; a coralline red alga, *Neogoniolithion* sp.*;* a tropical urchin, *Eucidaris tribuloides*; a temperate urchin, *Arbacia punctulata*; a serpulid worm, *Hydroides crucigera;* and an American oyster, *Crassostrea virginica*) that were reared for 60 days in isothermal seawater (25°C) equilibrated with an atmospheric pCO_2 of *ca.* 409 µatm. We observe large inter-species variability in $\delta^{11}B_{CaCO3}$ (*ca.* 20 ‰) and significant discrepancies between measured $\delta^{11}B_{CaCO3}$ and $\delta^{11}B_{CaCO3}$ expected from established relationships between $\delta^{11}B_{CaCO3}$ and seawater pH. We discuss these results in the context of various proposed mechanisms of biocalcification, including the potential dominant role that internal calcifying site pH plays in regulating $CaCO_3$ saturation state and borate $\delta^{11}B$ at the site of calcification and, thus, the $\delta^{11}B$ composition of calcifers' shells and skeletons.

1 Introduction

The ability to monitor historical changes in seawater pH on both short and long-term timescales is necessary to understand the influence that dramatic changes in atmospheric CO_2 (pCO_2) have had on marine carbonate chemistry. The recent anthropogenic increase in pCO_2 has already resulted in a significant decrease in seawater pH (IPCC, 2014), with potential effects on the ability of calcifying organisms to produce skeletal calcium carbonate ($CaCO_3$; IPCC, 2014). Ocean acidification studies have found that organismal responses vary between taxa, highlighting the complexity of biological responses to ocean acidification (Ries et al., 2009; Kroeker et al., 2010; Kroeker et al., 2013) and necessitating a more complete understanding of the various mechanisms of biocalcification governing organismal responses to ocean acidification.

Biogeosciences Discuss., doi:10.5194/bg-2017-154, 2017
Manuscript under review for journal Biogeosciences
Discussion started: 15 May 2017
© Author(s) 2017. CC-BY 3.0 License.

1.1 Theoretical model of $\delta^{11}B$ variation with pH

The boron isotope composition ($\delta^{11}B$) of biogenic $CaCO_3$ ($\delta^{11}B_{CaCO3}$) has been primarily used as a palaeoceanographic proxy for seawater pH (Hönisch and Hemming, 2004; Hönisch et al., 2004; Montagna et al., 2007; Palmer, 1998; Pearson et al., 2009; Penman and Hönisch, 2014; Rae et al., 2011; Saenger et al., 2013; Trotter et al., 2011; Vengosh et al., 1991; Wei et al., 2009; Zinke et al., 2014). Boron has a residence time in seawater of *ca.* 14 million years (Lemarchand et al., 2000), which is much longer than the mixing time of oceans (*ca.* 1000 years), suggesting that it behaves conservatively in time and space (Foster et al., 2010), making $\delta^{11}B$ an attractive palaeo-proxy for pH. The development of this proxy is based on a theoretical model of $\delta^{11}B$ variation with pH that assumes that $\delta^{11}B_{CaCO3}$ reflects the $\delta^{11}B$ composition of borate in seawater ($\delta^{11}B_{SW}$; Pagani et al., 2005). The theoretical model of $\delta^{11}B$ variation as a function of pH requires knowledge of the fractionation factor (α) for isotope exchange between the aqueous species of boron, the dissociation constant (pK_B), and the isotopic composition of boron in seawater (Pagani et al., 2005).

Boron exists in aqueous solutions as either trigonal boric acid [$B(OH)_3$] or as the tetrahedral borate anion [$B(OH)_4^-$] and their proportions in solution are pH dependent (Fig. 1), as defined by the following equilibrium reaction:

$$B(OH)_3 + H_2O \leftrightarrow B(OH)_4^- + H^+$$

In modern seawater, $B(OH)_4$ represents ~24.15 % of boron species, assuming that the dissociation constant (pK_B) between these two species of boron is 8.597 (at 25 °C, pH = 8.1; Dickson, 1990). Boron has two stable isotopes (^{10}B and ^{11}B) with relative abundances of 19.9 % and 80.1 %, respectively, and $B(OH)_3$ is enriched in ^{11}B relative to $B(OH)_4^-$ due to molecular differences of these chemical species in solution. The isotopic composition of boron is noted following standard convention:

$$\delta^{11}B = [(^{11}B_{sample}/^{10}B_{sample})/(^{11}B_{standard}/^{10}B_{standard})-1] \times 1000\ (‰); \quad (1)$$

where the reference standard is NIST SRM 951 (NIST, Gaithersburg, MD, USA).

The $\delta^{11}B$ of modern seawater is 39.61 ± 0.04 ‰ (Foster et al., 2010) and a large (> 20‰) and consistent fractionation of $\delta^{11}B$ exists between the two aqueous species described above. The fractionation between boric acid and borate ion is defined as:

$$\alpha \equiv \frac{(11B/10B)_{Boric\ acid}}{(11B/10B)_{Borate\ ion}};$$

A wide range of theoretical and empirical values for the fractionation factor between boric acid and borate ion in seawater (α) have been suggested (Byrne et al., 2006; Kakihana et al., 1977; Klochko et al., 2006; Nir et al., 2015; Palmer et al., 1987). For example, α = 1.0194 was calculated from theory by Kakihana et al. (1977) and has been widely applied in palaeo-reconstructions of seawater pH (Hönisch et al., 2004; Kakihana et al., 1977; Sanyal et al., 1995). Zeebe (2005) used analytical techniques and *ab initio* molecular orbital theory to calculate α ranging from 1.020 to 1.050 at 300 K. Zeebe (2005) provided several arguments in support of $\alpha \geqq 1.030$, ultimately concluding that experimental work was required to determine the α between dissolved boric acid and the borate ion. Subsequent to the work by Zeebe (2005), significant error was identified for the borate vibrational spectrum term used in Kakihana et al.'s (1977) theoretical calculation of α (Klochko et al., 2006; Rustad and Bylaska, 2007). An empirical α of 1.0272 (Klochko et al., 2006), using a corrected borate vibrational spectrum term, is now considered to best describe the boron isotope fractionation between dissolved boric acid and borate ion in seawater (Rollion-Bard and Erez, 2010; Xiao et al., 2014). Moreover, due to the ability of some calcifying organisms to alter carbonate chemistry at their site of calcification, and/or potential isotopic fractionation during boron incorporation in

Biogeosciences Discuss., doi:10.5194/bg-2017-154, 2017
Manuscript under review for journal Biogeosciences
Discussion started: 15 May 2017
© Author(s) 2017. CC-BY 3.0 License.

biogenic carbonates, species-specific fractionation factors and transfer functions are likely more appropriate than theoretical α values (Anagnostou et al., 2012; Hönisch et al., 2004; Krief et al., 2010; Rae et al., 2011; Reynaud et al., 2004; Trotter et al., 2011).

The $\delta^{11}B_{CaCO3}$ appears to be inherited from the $\delta^{11}B$ composition of dissolved $B(OH)_4^-$ in the solution from which that $CaCO_3$ precipitates, thereby quantitatively reflecting the pH of the precipitating solution. Experimental work (e.g., Hemming and Hanson, 1992; Sanyal et al., 2000) suggests that $B(OH)_4^-$ is the dominant species of dissolved inorganic boron incorporated into $CaCO_3$ minerals as they precipitate from solution. It is also well established that $\delta^{11}B$ of $B(OH)_4^-$ is controlled by solution pH (c.f. Hemming and Hönisch, 2007; see discussion above). Therefore, the $\delta^{11}B_{CaCO3}$ should reflect the pH of the precipitating solution. This has been demonstrated empirically in numerous studies (see Hemming and Hönisch, 2007, for summary). It should be noted that alternative models of boron incorporation into $CaCO_3$ have been proposed (Klochko et al., 2009), although most published studies rely upon the framework first proposed by Hemming and Hanson (1992).

1.2 The role of calcification site pH in calcareous biomineralization and organisms' responses to ocean acidification

The decrease in seawater pH that will accompany the forecasted rise in anthropogenic atmospheric pCO_2 will reduce seawater [CO_3^{2-}], which has been shown to inhibit biological deposition of $CaCO_3$, or even promote its dissolution (c.f. Doney et al., 2009; Fabry et al., 2008; Kleypas et al., 2006; Kroeker et al. 2010; Langdon, 2002; Ries et al., 2009). However, if seawater is the source of an organism's calcifying fluid (e.g., Gaetani and Cohen, 2006), then the concentration of dissolved inorganic carbon (DIC) in this fluid will increase as atmospheric pCO_2 increases. Organisms able to strongly regulate the pH of their calcifying fluid, despite reduced external pH, should convert much of this increased DIC, occurring primarily as HCO_3^-, back into the CO_3^{2-} that they need for calcification (Ries, 2011a, 2011b; Ries et al., 2009). Thus, an organism's specific response to CO_2-induced ocean acidification is critically dependent upon that organisms' ability to maintain an elevated pH at their site of calcification.

It should be noted that marine calcifiers biomineralize in diverse ways, and that some calcifers' mechanisms of biomineralization are better understood than others. Corals are thought to accrete $CaCO_3$ directly from a discrete calcifying fluid (e.g., Cohen and McConnaughey, 2003 and references therein; Al-Horani et al., 2003; Cohen and Holcomb, 2009; Gaetani and Cohen, 2006; Ries, 2011a), with mineralization sites and crystal orientations being influenced by organic templates and/or calicoblastic cells (e.g., Cuif and Dauphin, 2005; Goldberg, 2001; Meibom et al., 2008; Tambutté et al., 2007). Mollusks are also thought to precipitate their shells from a discrete calcifying fluid between the external epithelium of the mantle and the inner layer of the shell known as the extrapallial fluid (e.g., Crenshaw, 1972), with hemocytes and organic templates playing a potentially important role in crystal nucleation (e.g., Mairie et al., 2012; Mount et al., 2004; Weiner et al., 1984). Coralline red algae, such as those belonging to the family Corallinaceae, are also thought to precipitate high-Mg calcite (and/or aragonite) crystals from an intercellular calcifying fluid (Simkiss and Wilbur, 1989). Notably, biomineralization by coralline red algae occurs primarily within the cell wall and often has a preferred crystal orientation, which is not typical of other calcifying algae (Simkiss and Wilbur, 1989). Echinoids, in contrast, are thought to initiate calcification on Ca_2^+-binding organic matrices within cellular vacuoles (Ameye et al., 1998).

Many calcifying marine organisms, including scleractinian corals (Al-Horani et al., 2003; Cohen and Holcomb, 2009; Cohen and McConnaughey, 2003; Holcomb et al., 2010; Ries, 2011a), coralline red algae (Borowitzka and Larkum, 1987; McConnaughey and Whelan, 1997), calcareous green algae (De Beer and Larkum, 2001; Borowitzka and Larkum, 1987; McConnaughey and Falk, 1991), foraminifera (Rink et al., 1998; Zeebe and Sanyal, 2002), and crabs (Cameron, 1985) are

Biogeosciences Discuss., doi:10.5194/bg-2017-154, 2017
Manuscript under review for journal Biogeosciences
Discussion started: 15 May 2017
© Author(s) 2017. CC-BY 3.0 License.

thought to facilitate precipitation of their skeletal or shell $CaCO_3$ by elevating pH at their site of calcification. The effect of pH on $CaCO_3$ chemistry at the site of calcification can be summarized by the following equilibrium reactions:

$H_2CO_3 \leftrightarrow HCO_3^- + H^+$

and

$HCO_3^- \leftrightarrow H^+ + CO_3^{2-}$;

which are respectively governed by the following stoichiometric dissociation constants:

$K^*_1 = [HCO_3^-][H^+]/[H_2CO_3]$

and

$K^*_2 = [CO_3^{2-}][H^+]/[HCO_3^-]$

Thus, reducing $[H^+]$ at the site of calcification shifts the carbonic acid system towards elevated $[CO_3^{2-}]$, thereby increasing $CaCO_3$ saturation state (Ω_{CaCO3}) following:

$\Omega_{CaCO3} = [Ca_2^+][CO_3^{2-}]/K^*_{sp}$

where K^*_{sp} is the stoichiometric solubility product of the appropriate $CaCO_3$ polymorph (e.g., calcite, aragonite, etc.).

Various mechanisms have been proposed for elevating pH at the site of calcification, including conventional H^+-channeling (McConnaughey and Falk, 1991), Ca_2^+-H^+ exchanging ATPase (Cohen and McConnaughey, 2003; McConnaughey and Falk, 1991; McConnaughey and Whelan, 1997), light-induced H^+-pumping (De Beer and Larkum, 2001), transcellular symporter and co-transporter H^+- solute shuttling (McConnaughey and Whelan, 1997), cellular extrusion of hydroxyl ions (OH^-) into the calcifying medium, and CO_2-consumption via photosynthesis (e.g., Borowitzka and Larkum, 1976).

Regardless of the exact composition (e.g., seawater vs. modified seawater) or nature (e.g., fluid vs. gel) of their calcifying media, or the specific mechanisms by which they produce their $CaCO_3$ (e.g., organic templates vs. cellular mediation vs. proton-pumps vs. Ca^{2+}-ATPase), an organism's ability to control pH at their site of calcification should strongly influence their ability to convert DIC into CO_3^{2-}, thereby impacting their specific calcification response to CO_2-induced ocean acidification.

1.4 Relationship between calcification site pH and $\delta^{11}B_{CaCO3}$

Organisms that precipitate $CaCO_3$ from a discrete calcifying fluid should record in their shells and skeletons $\delta^{11}B_{CaCO3}$ compositions that reflect pH of their calcifying fluid. Numerous studies have documented a relationship between the pH of seawater and the $\delta^{11}B_{CaCO3}$ composition of foraminiferal shells and coral skeletons (Fig. 2). However, the observed relationships between biogenic $\delta^{11}B_{CaCO3}$ and seawater pH vary widely amongst taxa (Fig. 2), and generally differ from that measured or derived theoretically for $B(OH)_4^-$ in seawater (Byrne et al., 2006; Klochko et al., 2006; Liu and Tossell, 2005; Zeebe, 2005) and from that observed in abiotically precipitated $CaCO_3$ (Sanyal et al., 2000).

One hypothesis for the discrepancies between the expected $\delta^{11}B_{CaCO3}$-pH relationship and that actually observed for biogenically precipitated $CaCO_3$ exists because most marine calcifiers are not precipitating their $CaCO_3$ directly from seawater, but rather from a discrete calcifying fluid with a pH that is substantially elevated relative to that of their external

Biogeosciences Discuss., doi:10.5194/bg-2017-154, 2017
Manuscript under review for journal Biogeosciences
Discussion started: 15 May 2017
© Author(s) 2017. CC-BY 3.0 License.

seawater. Prior studies have shown that, for a given seawater pH, $\delta^{11}B_{CaCO3}$ of the coral species *Porites cylindrica* and *Acropora nobilis* is moderately elevated relative to $\delta^{11}B_{CaCO3}$ of the foraminifera *Globigerinoides sacculifer* and substantially elevated relative to the mollusk *Mytilus edulis* (Fig. 2; Heinemann et al., 2012; Hönisch et al., 2004; Sanyal et al., 2001). One possible explanation for these differences is that corals are maintaining their calcifying fluids at higher pH than the calcifying fluids of foraminifera, which are in turn elevated relative to the calcifying fluid pH of mussels. This is consistent with pH microelectrode (Al-Horani et al., 2003; Ries, 2011a), boron isotope (e.g., Anagnostou et al., 2012; Krief et al., 2010; Trotter et al., 2011; McCulloch et al., 2012; Wall et al., 2016), and fluorescent pH dye data (Venn et al., 2009, 2011, 2013) suggesting that scleractinian corals elevate their calcifying fluid pH to 8.5 – 10, versus their external seawater pH of 8, that foraminifera maintain their calcifying fluid pH between 8 and 9 (Rink et al., 1998), and that bivalves maintain their extrapallial fluid pH between 7.5 and 8 (Crenshaw, 1972).

Here, we investigate differences in $\delta^{11}B_{CaCO3}$-pH relationships amongst taxonomically diverse biogenic calcification systems and discuss the compatibility of these observations with the hypothesis that $\delta^{11}B_{CaCO3}$ of biogenic carbonate is recording pH of the organisms' calcifying fluids (rather than the organism's surrounding seawater)—a key parameter of biological calcification that has proven challenging to measure yet is fundamental to understanding, and even predicting, marine calcifiers' responses to CO_2-induced ocean. By systematically investigating the $\delta^{11}B_{CaCO3}$ composition of a taxonomically broad range of taxa, each employing different mechanisms of calcification, yet all cultured under equivalent laboratory conditions (Ries et al., 2009), we are able to empirically assess biological controls on the $\delta^{11}B_{CaCO3}$ composition of biogenic carbonates.

In this study, we evaluated the $\delta^{11}B_{CaCO3}$ of 6 highly divergent species of marine calcifiers reared for 60 days in isothermal (25°C) and isosaline (32 practical salinity units; psu) seawater equilibrated with atmospheric pCO_2 of *ca.* 409 µatm, including a temperate coral (*Oculina arbuscula*), a coralline red alga (*Neogoniolithion* sp.), a tropical urchin (*Eucidaris tribuloides*), a temperate urchin (*Arbacia punctulata*), a serpulid worm (*Hydroides crucigera*), and an American oyster (*Crassostrea virginica*). Three modern marine carbonate standards were also analysed as part of our $\delta^{11}B$ method validation, including: two corals (*Porites* sp.*;* JCp-1 from the Geological Survey of Japan; NEP, an internal standard from the University of Western Australia/Australian National University, McCulloch et al., 2014); and a giant clam (*Tridacna gigas;* JCt-1 from the Geological Survey of Japan).

2 Methods and materials

2.1 Laboratory conditions

Sample processing and chemical separation were performed under ISO 5 (class 100) laminar flow hoods within an ISO 6 (class 1,000) clean room at Ifremer (Plouzané, France). Analyses of $^{11}B/^{10}B$ ratios were carried out using a Thermo Scientific Neptune MC-ICP-MS at the Pôle spectrometrie Océan (PSO), Ifremer (Plouzané, France). Efforts were made to minimize sample exposure to laboratory air.

2.2 Reagents

Ultra-pure reagents were used for all chemical procedures. The source of high-purity water (UHQ) for the procedure is a Millipore Direct-Q water purification system with a specific resistivity of 18.2 MΩ·cm. All HNO_3 solutions are obtained from dilutions using Aristar Ultra high purity acid. The 0.5 N NH_4OH solutions are boron-cleaned by exchange with boron-specific resin (Amberlite IRA 743). UHQ water is buffered to pH 7 with the boron-cleaned NH_4OH. The reagent boron blanks were measured on a Thermo Scientific Element XR at the PSO, Ifremer (Plouzané, France) and were all < 0.1 ppb, yielding a total B blank of <100 ng per sample.

Biogeosciences Discuss., doi:10.5194/bg-2017-154, 2017
Manuscript under review for journal Biogeosciences
Discussion started: 15 May 2017
© Author(s) 2017. CC-BY 3.0 License.

185 **2.3 Standards**

A range of standards were used in this study, including: (1) the reference standard NIST SRM 951 (NIST, Gaithersburg, MD, USA) for B isotope ratio and B concentration; (2) a mixture of NIST SRM 951 and a series of ICPMS SRM for B:Ca ratio (30-200 µg/mg); (3) the international coral standard (*Porites* sp.) JCp-1 (Geological Survey of Japan, Tsukuba, Japan); (4) the international giant clam standard (*Tridacna gigas*) JCt-1 (Geological Survey of Japan, Tsukuba, Japan); and (5) NEP
190 internal coral standard *(Porites* sp.) from University of Western Australia/Australian National University.

2.4 Boron extraction procedure

Prior to boron isotope analysis, B was separated from the sample matrix using a B-specific anionic exchange resin (Amberlite IRA-743; Kiss, 1988). Amberlite IRA 743 behaves as an anion exchanger with a high affinity for B absorption at neutral to alkaline pH (i.e., will absorb B), and a low affinity for boron at acidic pH (i.e., will release B). The resin was
195 crushed and sieved to a desired 100 – 200 mesh, then cleaned and conditioned to a pH of 7 (6.8 – 7.2).

Here, we present two methods of B extraction (batch and column chemistry), where the influence of matrix chemistry is removed through minor adjustments to the chemistry of existing B extraction techniques. These two methods were applied to various biogenic $CaCO_3$ samples (*Porites* coral, temperate urchin, giant clam, American oyster). All samples are cleaned with an oxidative cleaning method (described in detail below) using NH_4OH-buffered H_2O_2 followed by multiple washes
200 with pH-buffered UHQ water (pH = 7).

2.4.1 Oxidative cleaning

Samples and reference materials JCp-1, JCt-1, and NEP were cleaned with an oxidative cleaning method following the method of Barker et al. (2003). For a 2 mg sample, 200 µL of the alkaline-buffered (0.1 M NH_4OH) H_2O_2 was added to remove organic matter. Samples were placed in an ultrasonicator for 20 minutes at 50 °C to expedite cleaning. Following
205 peroxide cleaning, samples were then submitted to multiple washes (typically 3) of UHQ water (pH = 7, 400 µL) until the pH of the supernatant matched that of the UHQ water to ensure removal of all oxidizing agent. The water was then removed from samples after centrifugation and a weak-acid leach was implemented by adding 20 µL of 0.001 M HNO_3 to each sample. Samples were then ultrasonicated for 10 minutes before the acid was removed and replaced with pH-buffered UHQ water. Dissolution of each sample was then performed by addition of 20 µL of 3 M HNO_3 followed by 300 µL of 0.05 M
210 HNO_3. The pH of each sample was then adjusted to pH 7 with 0.2 M NH_4OH, following partition coefficients for the B-specific resin reported by Lemarchand et al. (2002). For both the batch and the column chemistry methods, the resin is pre-cleaned and conditioned to a pH of 7 prior to sample loading.

2.4.2 Column chemistry method

A column chemistry protocol for B extraction (described in table 1) was developed based on methods described by Wang et
215 al. (2010) and Foster et al. (2013). Briefly, the columns were washed with pH-buffered MQ-H_2O (pH=7), 0.5 M HNO_3, and again with pH-buffered MQ-H_2O. The eluent was measured to ensure that it was at pH 7 prior to loading of the sample. The sample was then loaded onto the resin and washed multiple times (1500 µL x 3) with pH-buffered UHQ in order to remove any cations, and then the B was eluted in 1000 µL of 0.5 M HNO_3. Column yields were greater than 95 % (Fig. 3) and elution tails of every sample were checked with an extra 500 µL acid rinse. In all cases, this tail represented less than 1 % of
220 B loaded. Boron concentrations of small aliquots of each sample were measured by single collector ICPMS prior to analysis, and the concentration of other elements of interest (Ca, Na, Ba, U) were also monitored in this aliquot and the final solution in order to confirm complete removal of the sample matrix.

© Author(s) 2017. CC-BY 3.0 License.

2.4.3 Batch method

The batch method approach to B separation was conducted under closed conditions in an attempt to reduce airborne B contamination. Cleaned samples (pH 7) were transferred into acid-cleaned microcentrifuge tubes (500 µL) containing 5 mg of resin, which is B-cleaned with 500 µL of 0.5 M HNO_3, and then rinsed with 500 µL of MQ water (buffered to pH 7 with 2 % NH_4OH) three times to elute the other cations in the matrix and achieve pH 7. Tubes were then capped and shaken for 15 minutes to promote exchange of anions from the aqueous sample to the resin. Afterwards, the mixture was centrifuged (1 min, 2000 rpm), the matrix was decanted, and the resin was washed three times (200 µL) with pH-buffered (pH 7) UHQ water to elute any cations. Boron recovery was then performed with the addition of 500 µL 0.05 M HNO_3 and shaken again for 15 min to promote the anion exchange between the resin and solution. A final tail-check was performed with 100 µL of 0.05 M HNO_3 to ensure that all of the B was recovered in the initial 500 µL 0.05 M HNO_3 solution.

2.5 Procedural blanks

The total yield of B from procedural blanks, which encompasses reagent, air-borne and procedural contamination, was sub-nanogram. Such low contamination was achieved through stringent cleaning and handling protocols for all consumables and reagents, thereby permitting accurate measurement of B at sub-µM concentrations.

2.6 Boron recovery and matrix removal

A major challenge in the measurement of $\delta^{11}B$ by MC-ICPMS is the elimination of residual boron from prior analyses (i.e., 'memory effects'). In order to evaluate memory effects, multiple concentrations (30 ppb to 130 ppb) of a standard solution (NIST 951) were analysed. After washing out the MC-ICPMS with a solution of 0.05 M HNO_3 for several minutes, the residual ^{11}B and ^{10}B signals were in the range of 10 – 80 mV, equivalent to 5 % (30 ppb) and 3 % (130 ppb), respectively (see Fig. S1 for ^{11}B blanks). Boron recovery was measured using a Thermo Scientific Element XR HR-ICP-MS at the Laboratory for Geochemistry and Metallogeny, Ifremer (Plouzané, France). Boron yields are evaluated by tracking B throughout the entire procedure.

2.7 Mass spectrometry

Isotopic measurements were conducted using a Thermo Scientific Neptune MC-ICPMS at the PSO, Ifremer (Plouzané, France), operated with standard plasma settings. To account for drift in mass discrimination through the analysis, samples were bracketed by matrix-matched standards of similar composition. Typically, the concentration of the standard (NIST SRM 951) was 50 ppb in 0.05 M HNO_3. Each analysis consisted of a 2-minute simultaneous collection of masses 11 and 10 on Faraday cups H3 and L3 equipped with 10^{11} Ω resistors. Each sample was analysed in duplicate during a single analytical session and the replicate analyses did not share a bracketing standard. As such, the boron isotope ratios are determined as delta values ($\delta^{11}B$). The $\delta^{11}B$ was also evaluated by analysing JCp-1 (*Porites* sp.), NEP (*Porites* sp.) and JCt-1 (hard clam) standards, which were processed in the same manner and reported relative to their reference values (Foster et al., 2013; McCulloch et al., 2014).

The MC-ICPMS method is a commonly used approach to measure $\delta^{11}B$ due to its capacity for rapid, accurate and reproducible analyses (McCulloch et al., 2014). Challenges with this method arise from the volatile and persistent nature of boron that can result in significant memory effects, cross-contamination between samples and standards, and unanticipated matrix effects (McCulloch et al. 2014; Foster et al. 2013). Given the sensitivity of $\delta^{11}B_{CaCO3}$-based estimates of calcification site pH to the analytical uncertainty cited above, two different injection methods (described below) were evaluated to determine what method is most suitable for minimizing analytical error.

Biogeosciences Discuss., doi:10.5194/bg-2017-154, 2017
Manuscript under review for journal Biogeosciences
Discussion started: 15 May 2017
© Author(s) 2017. CC-BY 3.0 License.

2.7.1 Demountable direct injection nebulizer

Memory effects were addressed by introducing samples to the plasma with demountable direct injection nebulizer (d-DIHEN; Louvat et al., 2014). Baseline B-concentrations between samples were measured with counting times of 30 s (Table 2).

2.7.2 Ammonia addition

For the ammonia addition method, a dual inlet PFA Teflon spray chamber was used with an ESI PFA 50 µL/min nebuliser to add ammonia gas at a rate of ~3 mL/min (Al-Ammar et al., 2000; Foster, 2008). The addition of ammonia gas to the spray chamber ensures that the analyte remains alkaline, which prevents volatile boron from recondensing in the chamber during analysis (Al-Ammar et al., 2000). The measured B signal of the rinse blank was then subtracted from the B isotope ratios in order to monitor B wash out, as suggested by Foster (2008). In all cases, wash out time was 200 seconds and samples were matrix- and intensity-matched to the bracketing standards.

3 Results

3.1 Method development

3.1.1 Yield and reproducibility

The yields for boron extraction for both methods were evaluated for various biogenic $CaCO_3$ samples and were typically between 97 and 102 % (determined by HR-ICPMS; see section 2.6). Washes with pH-buffered MQ-H_2O effectively removed Ca (99.9 %), Na (100 %), Ba (> 80 %), and U (> 93 %) from the sample matrix. The robustness of the methods is demonstrated by the observed agreement between measured values of the international $CaCO_3$ standards JCp-1 and JCt-1, a coral (*Porites* sp.; $\delta^{11}B_{NH3}$ = 24.45 ± 0.28 ‰, $\delta^{11}B_{d\text{-}DIHEN}$ = 24.30 ± 0.16 ‰) and a giant clam (*Tridacna gigas*; $\delta^{11}B = 16.65_{NH3}$ ± 0.39 ‰, $\delta^{11}B_{d\text{-}DIHEN}$ = 17.5 ± 0.60 ‰), and their values established via inter-laboratory calibration ($\delta^{11}B$ = 24.36 ± 0.51 ‰, n = 10 and 16.34 +/- 0.64 ‰, respectively; Gutjahr et al. 2014; see Table 3). In addition, both column and batch methods were evaluated using the NEP internal standard (*Porites* sp.), a temperate urchin, a hard clam, and an oyster. As shown in Table 3, good agreement was achieved between $\delta^{11}B_{CaCO3}$ obtained via the batch and column chemistry methods for each of the biogenic $CaCO_3$ samples analysed.

3.1.2 Extraction blanks, boron recovery, and matrix removal

See sections 2.5 and 2.6.

3.2 Boron isotope composition of marine biogenic $CaCO_3$

Average $\delta^{11}B_{CaCO3}$ composition for all species evaluated in this study range from 16.27 ‰ to 35.09 ‰ (Table 3). The individual and average data are presented in Tables 3 and 4, respectively, and summarized in the text that follows. The coralline red alga *Neogoniolithion* sp. (35.89 ± 3.71 ‰; n = 3) exhibited the highest $\delta^{11}B_{CaCO3}$, followed by the temperate coral *O. arbuscula* (24.12 ± 0.19 ‰; n = 3), the tube of the serpulid worm *H. crucigera* (19.26 ± 0.16 ‰; n = 3), the tropical urchin *E. tribuloides* (18.71 ± 0.26 ‰; n = 3), the temperate urchin *A. punctulata* (16.28 ± 0.86 ‰; n = 3), and the American oyster *C. virginica* (16.03 ‰; n = 1). Therefore, a range of *ca.* 20 ‰ in $\delta^{11}B_{CaCO3}$ was observed across all species evaluated in this study (Table 3 and 4). Notably, these are the first published $\delta^{11}B_{CaCO3}$ data for serpulid worm tubes and oysters.

Biogeosciences Discuss., doi:10.5194/bg-2017-154, 2017
Manuscript under review for journal Biogeosciences
Discussion started: 15 May 2017
© Author(s) 2017. CC-BY 3.0 License.

3.3 Compatibility of the interspecific range of $\delta^{11}B_{CaCO3}$ with established seawater borate $\delta^{11}B$-pH relationships

Because the investigated organisms were cultured under relatively equivalent conditions (pCO_2 of 409 ± 6 µatm, 32 ± 0.2 psu, 25 ± 0.1 °C; see Ries et al. 2009), differences in seawater pH could not have been a significant driver of the observed interspecific variability in $\delta^{11}B_{CaCO3}$ (*ca.* 20 ‰; Tables 3 and 4). In order to evaluate this *ca.* 20 ‰ interspecific variability in $\delta^{11}B$, the data are plotted against measured seawater pH and graphically compared with theoretical borate $\delta^{11}B$-pH curves often used to interpret $\delta^{11}B_{CaCO3}$ data in the context of seawater pH (Fig. 4). Clear offsets from the seawater borate $\delta^{11}B$-pH curve (Klochko et al., 2006) can be observed for several of the species: the temperate coral (*O. arbuscula*) and coralline red alga (*Neogoniolithion* sp.) fall above the curve, the temperate urchin (*A. punctulata*) and American oyster (*C. virginica*) fall below the curve, and the tube of the serpulid worm (*H. crucigera*) and the tropical urchin (*E. tribuloides*) fall nearly on the curve (see Fig. 4 and Table 3). The interpretation of these offsets from the seawater borate $\delta^{11}B$-pH curve is discussed below.

4 Discussion

4.1 Appropriateness of method for analysing $\delta^{11}B_{CaCO3}$ in marine $CaCO_3$ samples

This study describes extensive method development and analytical validation used to establish stable boron isotope measurements at Ifremer (Plouzané, France), including comparisons of different techniques for sample preparation and sample introduction to the mass spectrometer. For each of the samples evaluated, neither cleaning protocol, nor method of sample preparation, nor injection system was found to cause a significant difference in $\delta^{11}B_{CaCO3}$ composition of the samples (Table 3). The most effective method for minimizing memory effects in our MC-ICPMS analyses was found to be d-DHIEN (Louvat *et al.*, 2011). However, d-DHIEN has a complicated set-up and often generates capillary blockages arising from the aspiration of particles (e.g., resin), and/or from plasma extinction resulting from air bubble introduction. In short, sample analysis via d-DHIEN requires nearly continuous use to maintain its stability. In contrast, the ammonia-addition method (Al-Ammar *et al.*, 1999, 2000) requires continuous attention by personnel while in use, due to the use of ammonia gas, but is set-up and disassembled with relative ease between uses. We found that a constant ammonia flow of 3 mL/min was necessary to maintain a sufficiently high pH to enable a fast rinse. Less than a 3 % boron memory effect was stable after 2 minutes, enabling a signal correction for the sample that follows. Both the column and batch method of B separation yielded low blanks when < 60 µL of resin was used (see sections 2.5 and 2.6). However, the batch method was identified as preferable over the column chemistry method since the batch method has a reduced risk of B contamination due to reduced contact time with air and the small volumes of both resin and acids used in the separation process.

4.2 The $\delta^{11}B_{CaCO3}$ compositions for a diverse range of marine calcifiers

The six species investigated exhibited a broad spectrum of $\delta^{11}B_{CaCO3}$ compositions, ranging from 16.03 ‰ to 35.89 ‰ (Table 4). Assuming that only the borate ion is incorporated into $CaCO_3$ structures, the wide variation in $\delta^{11}B_{CaCO3}$ (*ca.* 20 ‰) amongst the investigated species, reared under equivalent thermo-chemical conditions, may arise from inherent differences in calcification site pH amongst the species. If this is the case, then the observed range in range in $\delta^{11}B_{CaCO3}$ amongst the species (16.03 ‰ to 35.89 ‰) translates to an approximate range in calcification site pH of 7.9 – 9.4.

Boron co-precipitation with inorganic $CaCO_3$ (i.e. abiogenic) is known to be dependent on solution pH and inorganic $CaCO_3$ precipitation rate, however, the relative abundances of the inorganic B species in solution that are incorporated into inorganic $CaCO_3$ (borate ion and boric acid) have been shown to be independent of the parent solution pH (Mavromatis et al. 2015). Although Mavromatis et al. (2015) also found that polymorph mineralogy influences both the B/Ca ratio (higher in aragonite than calcite) and speciation of B in inorganic $CaCO_3$ (borate/boric acid ratio higher in aragonite than calcite), polymorph

© Author(s) 2017. CC-BY 3.0 License.

mineralogy was not found to influence boron isotope fractionation (Noireaux et al. 2015). Furthermore, because the borate/boric acid ratio is higher in aragonite than in calcite, aragonite-producing species should have a universally lower $\delta^{11}B_{CaCO3}$ composition than calcite-producing species (urchins, coralline alga, oyster) if shell mineralogy was the primary driver of the observed interspecific variation in $\delta^{11}B_{CaCO3}$ compositions – a trend that is not observed (Fig. 5). Thus, interspecific differences in polymorph mineralogy cannot, alone, explain the species' disparate $\delta^{11}B_{CaCO3}$ compositions. The more parsimonious explanation for these observed differences in $\delta^{11}B_{CaCO3}$ appears to be differences in pH at the site of calcification, which would change the speciation of dissolved B at the site of calcification, and therefore the isotopic composition of the borate ion that is preferentially incorporated into the organisms' $CaCO_3$.

Significant deviations from equilibrium exist in the isotope composition (e.g. O, C, B) of biogenic marine $CaCO_3$ (e.g., Hemming and Hanson, 1992; McConnaughey, 1989). Notably, many marine calcifiers have $\delta^{11}B$ values that differ from the $\delta^{11}B$ composition of borate ions dissolved in seawater at an equivalent pH (Figs. 3 and 5). When interpreted in the context of the framework that skeletal $\delta^{11}B$ reflects calcification site pH rather than pH of the organism's surrounding seawater, these results suggest that marine calcifiers are precipitating their $CaCO_2$ from a discrete fluid with a pH higher than, equal to, or, for some species, below that of seawater. A second hypothesis is that whilst seawater pH exerts some control over borate $\delta^{11}B$ at the site of calcification and, hence, $\delta^{11}B_{CaCO3}$, there are other species-specific effects that may influence $\delta^{11}B_{CaCO3}$ composition. The compatibility of these two hypotheses with existing models of biomineralization and observed $\delta^{11}B_{CaCO3}$ for the various marine calcifiers investigated in the present study are discussed below.

4.2.1 Temperate coral

The average $\delta^{11}B_{CaCO3}$ for the temperate coral *O. arbuscula* evaluated in this study (24.12 ± 0.19 ‰; n = 3; Tables 3 and 4) is similar to other literature-based values determined for aragonitic corals (Table 5; see references therein). Generally, aragonitic corals are enriched in ^{11}B when compared with a theoretical borate $\delta^{11}B$-pH curve (see Figures 3 and 5). The main vital effect typically used to describe ^{11}B-enrichment in corals, relative to seawater, is an increase in calcifying fluid pH at the coral's site of calcification (e.g., Rollion-Bard et al., 2011b; Trotter et al., 2011; Anagnostou et al., 2012; McCulloch et al., 2012). This hypothesis is supported by *in situ* measurements of pH using microelectrodes (e.g., Al-Horani et al., 2003; Ries, 2011), boron isotope analyses (e.g., Anagnostou et al., 2012; Krief et al., 2010; Trotter et al., 2011; McCulloch et al., 2012; Wall et al., 2016), and fluorescent pH dye data (Venn et al., 2009, 2011, 2013).

4.2.2 Coralline red alga

The average $\delta^{11}B_{CaCO3}$ for the branching, nonarticulated coralline red alga *Neogoniolithion* sp. evaluated in this study (35.89 ± 3.71 ‰; n = 3; Tables 3 and 4) is higher than the $\delta^{11}B_{CaCO3}$ composition of any other calcifying marine organism evaluated to date (Table 5). Of particular interest, one of the coralline red alga specimens evaluated in this study exhibited $\delta^{11}B_{CaCO3}$ (39.94 ‰, Table 3) similar to the average $\delta^{11}B_{SW}$ value (i.e., comprising the $\delta^{11}B$ composition of both dissolved borate and boric acid; 39.61 ‰) determined by Foster et al. (2010), raising the possibility that coralline red alga incorporate both species of dissolved inorganic boron during calcification. In support of this argument, Cusack et al. (2015) provide NMR data indicating that 30 % of the B incorporated into the coralline red alga *Lithothamnion glaciale* was present as boric acid. However, since the coralline red algae were reared at a pH of 8.1, the $\delta^{11}B_{CaCO3}$ compositions observed for the coralline algae in the present study would require incorporation of both inorganic species of boron at $[B(OH)_3]$:$[B(OH)_4^-]$ ratios of ca. 75:25, not the 30:70 ratio observed by Cusack et al. (2015). Alternatively, $\delta^{11}B_{CaCO3}$ compositions of coralline red algae data may reflect an elevated pH at the site of calcification (9.4; Table 4, Fig. 4), suggesting that coralline red algae are highly

Biogeosciences Discuss., doi:10.5194/bg-2017-154, 2017
Manuscript under review for journal Biogeosciences
Discussion started: 15 May 2017
© Author(s) 2017. CC-BY 3.0 License.

efficient at removing protons from their calcifying medium. Yet another explanation is that $\delta^{11}B_{CaCO3}$ of coralline algae is reflecting elevated pH at the alga's seawater boundary layer, driven by the alga's photosynthetic drawdown of aqueous CO_2.

4.2.3 Tropical and temperate urchins

The average $\delta^{11}B_{CaCO3}$ for the tropical urchin *E. tribuloids* (18.71 ± 0.26 ‰; n = 3; Tables 3 and 4) and for the temperate urchin (*A. punctulata*; 16.28 ± 0.86 ‰; n = 3; Tables 3 and 4), both evaluated in this study and reared at equivalent seawater conditions (pH = 8.0; 25 °C; 32 psu; Table 4), are less than $\delta^{11}B_{CaCO3}$ previously reported for other echinoid species (see Table 4; 22.7 ‰ - 22.8 ‰) but are close to theoretical values of dissolved borate at those seawater conditions (17.33 ‰; Fig. 4). Micro-electrode evidence suggests that urchins calcify using fluids with a pH and composition similar to that of seawater (Stumpp et al. 2012), which is supported by our observation that urchin $\delta^{11}B_{CaCO3}$ is similar to $\delta^{11}B$ of dissolved borate. The difference between the $\delta^{11}B_{CaCO3}$ of these two species of urchin and the calculated $\delta^{11}B_{CaCO3}$ (17.33 ‰) is +1.38 ‰ for the tropical urchin and -1.05 ‰ for the temperate urchin – a difference that exceeds their interspecimen variability (± 0.26 ‰ for the tropical urchin; ± 0.86 ‰ for the temperate urchin, determined as standard deviation (SD), see Table 5). However, the urchins could achieve this deviation in $\delta^{11}B_{CaCO3}$ by adjusting pH of their calcifying environment by only ± 0.1 units (e.g., calcification site pH of 8.1 and 7.9 yield $\delta^{11}B$ of calcification site borate of 18.38‰ and 16.42 ‰, respectively; see table 4). Thus, if deviations in urchin $\delta^{11}B_{CaCO3}$ from seawater borate $\delta^{11}B$ indeed reflect urchins' ability to modify pH at their site of calcification, these modifications appear to be relatively minor (i.e., ± 0.1 pH units) and not always in a direction that favours calcification—consistent with Stumpp et al.'s (2012) observation that urchin biomineralization can occur in cellular compartments where pH is lower than that of seawater.

4.2.4 Serpulid worm tube

The average $\delta^{11}B_{CaCO3}$ for the calcareous tube of the serpulid worm *H. crucigera* evaluated in this study (19.26 ± 0.16 ‰; n = 3; Tables 3 and 4) is close to theoretical values of $\delta^{11}B$ for seawater borate (Fig. 4). Serpulid worms secrete calcareous tubes with *H. crucigera* being the only species that secretes a combination of aragonite and high-Mg calcite (HMC; Ries, 2011b). In order to produce their calcareous tubes, *H. crucigera* produces a slurry of $CaCO_3$ granules in a pair of anterior glands, which coalesces within a matrix of inorganic and organic components (Hedley, 1956). The samples of *H. crucigera* evaluated in this study were exposed to environmental conditions (pH = 8.1; 25 °C; 32 psu; Table 4) yielding a theoretical seawater borate $\delta^{11}B$ and, thus, $\delta^{11}B_{CaCO3}$ of 18.38 ‰, which is 0.88 ‰ less than $\delta^{11}B_{CaCO3}$ measured for *H. crucigera.* Similar to the tropical urchin discussed above, the serpulid worm could generate this divergence in $\delta^{11}B_{CaCO3}$ from seawater borate $\delta^{11}B$ by elevating pH at its site of calcification by 0.08 units relative to pH_{SW}. It should be noted that by producing their tubes from a mixture of aragonite and HMC, serpulid worm biomineralization and the resulting $CaCO_3$ matrix is fundamentally different than that of the other marine calcifiers evaluated in this study, which are predominantly monomineralic. Notably, these are the first published $\delta^{11}B_{CaCO3}$ data for serpulid worm tubes.

4.2.5 American oyster

The $\delta^{11}B_{CaCO3}$ for the American oyster *C. virginica* evaluated in this study (16.03 ‰; n = 1; Tables 3 and 4) is less than the theoretical values of $\delta^{11}B$ for seawater borate (Fig. 4). Mollusks, such as oysters, construct their shells of LMC (aragonite during the larval stage) from a discrete calcifying fluid known as the extrapallial fluid ('EPF'; e.g., Crenshaw, 1972), with hemocytes and organic templates playing a potentially important role in crystal nucleation (e.g., Wilbur and Saleuddin 1983; Wheeler 1992; Marie et al., 2012; Weiner et al., 1984; Mount et al., 2004).). The sample of *C. virginica* evaluated in this study was exposed to seawater conditions (pH = 8.2; 25 °C; 32 psu; Table 4) that yield a theoretical borate $\delta^{11}B$, and thus

© Author(s) 2017. CC-BY 3.0 License.

410 $\delta^{11}B_{CaCO3}$, of 19.57 ‰, which is 3.54 ‰ greater than $\delta^{11}B_{CaCO3}$ measured for *C. virginica.* The observation that oyster $\delta^{11}B_{CaCO3}$ is substantially less than theoretical $\delta^{11}B$ of seawater borate suggests that pH of oyster extrapallial fluid pH is less than the pH of the oyster's surrounding seawater. Indeed, pH microelectrode measurements show that pH of oyster EPF (pH_{EPF}) is approximately 0.5 units less than seawater pH, which the author attributes to metabolically driven accumulation of dissolved CO_2 when the oyster's shell is closed (Crenshaw, 1972; Littlewood and Young, 1994; Michaelidis et al., 2005).
415 Oysters appear to overcome low $CaCO_3$ saturation state in the EPF, compared to corals that maintain elevated $CaCO_3$ saturation state at their site of calcification, by using organic templates to facilitate biomineral growth (e.g., Marie et al., 2012; Addadi et al., 2003; Weiner et al., 1984). The oyster could generate this negative divergence in $\delta^{11}B_{CaCO3}$ from seawater borate $\delta^{11}B$ by decreasing pH at the site of calcification by 0.35 units (Table 4), which, given the proximity of the independent pH-microelectrode measurements of oyster EPF, seems to be a plausible explanation for why oyster $\delta^{11}B_{CaCO3}$
420 falls below the theoretical borate $\delta^{11}B$-pH curve (Klochko; 2009; Fig 6). Notably, these are the first published $\delta^{11}B_{CaCO3}$ data for oysters.

4.3 What does a species' $\delta^{11}B_{CaCO3}$ reveal about its calcification site pH and relative sensitivity to ocean acidification?

Understanding how marine organisms calcify is a critical requirement for understanding and, ideally, predicting their physiological responses to future ocean acidification (e.g., Kleypas et al., 2006). Given that all 6 species were grown under
425 nearly equivalent controlled laboratory conditions, the observed interspecific range in $\delta^{11}B_{CaCO3}$ supports the hypothesis that B-isotope fractionation in marine calcifiers is species-dependent (see Table 5 and references therein). We hypothesize that this species-dependent variability is driven by interspecific differences in pH at the site of calcification. To explore this hypothesis, $\delta^{11}B_{CaCO3}$ values were converted to calcification site pH (pH_{CS}) from measured seawater temperature, salinity, seawater $\delta^{11}B$ value of 39.61 ± 0.04 ‰ (Foster et al., 2010), and a B-isotope fractionation factor of 1.0272 (Klochko et al.,
430 2006; Table 4). These calculations yield a calcification site pH (see Table 4) of 8.5 for the temperate coral (*O. arbuscula*), 9.4 for the coralline red alga (*Neogoniolithion* sp.), 8.1 for the tropical urchin *(E. tribuloides*), 7.9 for the temperate urchin (*A. punctulata*), 8.2 for the serpulid worm (*H. crucigera*), and 7.9 for the American oyster (*C. virginica*). Notably, the temperature coral (*O. arbuscula*) and coralline red alga (*Neogoniolithion* sp.) have higher calculated calcification site pH (based on their boron isotope composition) than the other organisms. As discussed above (section 4.2), one possible
435 explanation for these differences is that corals (and potentially coralline red algae) maintain their calcifying fluids at a higher pH than the calcifying fluids of other calcifying marine organisms.

Notably, the different species' $\delta^{11}B_{CaCO3}$ and reconstructed calcification site pH appeared to exhibit a moderate, inverse relationship with their experimentally determined vulnerability to ocean acidification (Ries et al., 2009)—i.e., species exhibiting more resilient 'parabolic' (e.g., coralline red alga) and 'threshold' (e.g., coral, tropical urchin) responses to ocean
440 acidification generally exhibited a higher $\delta^{11}B_{CaCO3}$ and, thus, calcification site pH than species exhibiting the more vulnerable 'negative' responses (e.g., oyster, serpulid worm) to ocean acidification (Table 4). The temperate urchin was the exception to this general trend, as it exhibited a relatively resilient parabolic response to ocean acidification yet maintained $\delta^{11}B_{CaCO3}$ and, thus, calcification site pH close to that of seawater.

In the absence of empirical measurements of calcifying fluid temperature, salinity, and $\delta^{11}B$, these parameters are generally
445 assumed to reflect seawater. However, the large variability in the calculated calcification site pH for these organisms (e.g. 7.9-9.4; Table 4) that were grown in near identical seawater conditions (pH = 8.0-8.2; Table 4) suggests that a biological process (e.g., regulation of calcification site pH) is governing boron isotope fractionation within the calcifying fluids and shells of marine calcifiers. Below, we evaluate the sensitivity of calculating calcification site pH from measured $\delta^{11}B_{CaCO3}$ composition by testing the factors that may influence the theoretical model of borate $\delta^{11}B$ variation as a function of pH;

© Author(s) 2017. CC-BY 3.0 License.

namely pK_B and α. A sensitivity analysis of $\delta^{11}B$ in seawater was not conducted since all organisms evaluated in this study were exposed to seawater from the same source and, thus, of identical $\delta^{11}B$ composition.

4.3.1 Sensitivity of $\delta^{11}B_{CaCO3}$ for estimating seawater and calcification site pH

Here, we explore the sensitivity of $\delta^{11}B_{CaCO3}$-derived determinations of pH, for both seawater and calcifying fluid, and the viability of theoretical borate $\delta^{11}B$-pH curves in applying the $\delta^{11}B$ palaeo-pH proxy.

The determination of pH from pK_B and the $\delta^{11}B$ of seawater and $B(OH)_4^-$ ($\delta^{11}B_{B(OH)4}$) can be summarized with the following equation (Eq. 1):

$$pH = pK_B - \log((\delta^{11}B_{SW} - \delta^{11}B_{B(OH)4})/(\delta^{11}B_{SW} - (\alpha \times \delta^{11}B_{B(OH)4}) - 1000(\alpha - 1))); \quad (1)$$

where pK_B is 8.6152 (at 25°C and 32 psu; Dickson, 1990), $\delta^{11}B_{SW}$ is 39.61 ‰ (Foster et al., 2010), and α is 1.0272 (Klochko et al., 2006). Thus, $\delta^{11}B_{B(OH)4}$, viz. $\delta^{11}B_{CaCO3}$, can be calculated across a range of pH_{SW} (Fig. 1b; Table S1).

It is important to note that the difference in $\delta^{11}B_{CaCO3}$ between each pH unit (when fluid pH < pK_B) increases with pH, as shown in Fig. 1b (see also Table S1). For example, a change in pH from 7.75 to 7.80 predicts a $\delta^{11}B_{CaCO3}$ difference of 0.35 ‰ (15.77 ‰ – 15.42 ‰), whereas a change in pH from 8.35 to 8.40 predicts a $\delta^{11}B_{CaCO3}$ difference of 0.74 ‰ (22.59 ‰ – 21.85 ‰). Thus, the relationship between fluid pH and $\delta^{11}B_{B(OH)4}$ is nonlinear over the range of fluid pH of interest (7 < pH < 10), with pH having the greatest influence on $\delta^{11}B_{B(OH)4}$, viz. $\delta^{11}B_{CaCO3}$, as fluid pH approaches pK_B.

As discussed above (section 4.2), most marine calcifiers are thought to precipitate $CaCO_3$ from a discrete 'calcifying fluid', which appears to be derived, yet physically separated, from seawater and has a pH greater than (e.g., coralline alga, corals), equivalent to (e.g., serpulid worm, urchins), or less than (e.g., oysters) seawater. Although the sensitivity analysis for the $\delta^{11}B_{CaCO3}$-derived determinations of pH at a pK_B of 8.6152 indicates that a small change in calcification site pH will greatly influence $\delta^{11}B_{CaCO3}$, especially as pH approaches pK_B (8.6152), the range of the organisms' seawater pH (8.0-8.2; Table 4) could only account for a theoretical 2.24 ‰ range in $\delta^{11}B_{CaCO3}$ (Table S1), far less than the ca. 20 ‰ range that was observed. It therefore follows that the large variability in $\delta^{11}B_{CaCO3}$ (*ca.* 20 ‰) observed for the investigated species requires an alternative explanation, such as changes in calcification site pH—particularly for the coralline alga, coral and oyster species that exhibited such large deviations in predicted vs. observed $\delta^{11}B_{CaCO3}$ (see section 4.2).

4.3.2 Sensitivity analysis of $\delta^{11}B$-derived pH to choice of α

As discussed in the Introduction (section 1.1), much work has gone into establishing a fractionation factor (α) that accurately describes the relationship between the $\delta^{11}B$ of dissolved borate and boric acid in seawater, and pH (see Xiao et al., 2014 for detailed discussion), with the earliest published palaeo-pH reconstructions using a theoretical value of 1.0194 (Kakihana, 1977; see Fig. 3). An empirical α of 1.0272 (Klochko et al., 2006) has now been shown to better predict borate $\delta^{11}B$, viz. $\delta^{11}B_{CaCO3}$, across a range of pH relevant for seawater (Rollion-Bard and Erez, 2010; Xiao et al., 2014). However, $\delta^{11}B_{CaCO3}$ of many species of calcifying marine organisms fall either above or below the theoretical borate $\delta^{11}B$-pH curves. It has long been suggested (and shown for corals) that calcifying organisms diverge from the predicted $\delta^{11}B_{CaCO3}$ due to their ability to modify pH of their calcifying environments (e.g., Anagnostou et al., 2012; Hönisch et al., 2004; Krief et al., 2010; Rae et al., 2011; Reynaud et al., 2004; Trotter et al., 2011; McCulloch et al., 2012). In the present study, species-specific divergences in $\delta^{11}B_{CaCO3}$ from the theoretical borate $\delta^{11}B$-pH curves are interpreted as evidence of modified pH at the organism's site of

© Author(s) 2017. CC-BY 3.0 License.

485 calcification. Importantly, existing models of biomineralization for each species are generally compatible with these $\delta^{11}B_{CaCO3}$-derived estimates of calcification site pH (see section 4.2).

Although an α of 1.0272 (Klochko et al., 2006) was used in the present study to estimate calcification site pH, other theoretical values for α, yielding slightly different borate δ^{11}B-pH curves (e.g., Byrne et al., 2006; Palmer et al., 1987; see Fig. 4), will of course yield slightly different estimates of pH at the calcification sites of each organism. For example, using
490 α values of 1.033 (Palmer et al. 1987), 1.0285 (Byrne et al. 2006), 1.0272 (Klochko et al. 2006), and 1.0194 (Kakihana et al. 1977) and a $\delta^{11}B_{CaCO3}$ of 24.12 ‰ (temperate coral; pH_{SW} = 8.1) yields calcification site pH of 8.7, 8.6, 8.5, and 8.1, respectively – a difference of 0.6 pH units. It should also be noted that the lower the $\delta^{11}B_{CaCO3}$, the more sensitive the reconstructed pH is to choice of α. For example, changing α from 1.0272 to 1.0330 will result in a 0.24 pH unit shift for $\delta^{11}B_{CaCO3}$ = 20 ‰, but only a 0.12 and 0.08 pH unit shift for $\delta^{11}B_{CaCO3}$ = 30 ‰ and 39.5 ‰, respectively. This underscores
495 the importance of using the same α when comparing calcification site pH amongst species.

4.3.3 Implications of $\delta^{11}B_{CaCO3}$-derived estimates of calcification site pH for species-specific vulnerability to ocean acidification

Regardless of which α value is used, a wide range (*ca.* 20 ‰) of $\delta^{11}B_{CaCO3}$ compositions is observed amongst the marine calcifying species investigated. Furthermore, there appears to be a moderate inverse relationship between the species'
500 relative ability to elevate calcification site pH and their empirically determined vulnerability to ocean acidification. These results support the assertion that interspecific differences in calcification site pH contribute to marine calcifiers' differential responses to ocean acidification – highlighting the need for future queries into the mechanisms driving boron isotope fractionation and biomineralization within marine calcifying organisms.

4.3.4 Further calibration of the $\delta^{11}B_{CaCO3}$-derived determinations of pH

505 The observed deviations of the investigated species' $\delta^{11}B_{CaCO3}$ from the borate δ^{11}B-pH curve also highlight that, in some species, paleo-seawater pH may not simply be reconstructed by projecting measured $\delta^{11}B_{CaCO3}$ onto a theoretical seawater borate δ^{11}B-pH curve. Instead, the model species used for paleo-seawater pH reconstructions may require calibration through controlled laboratory experiments and/or core-top calibrations that empirically define the species-specific relationship between seawater pH and $\delta^{11}B_{CaCO3}$.

510 ## 5 Conclusion

This study establishes the methodology for measuring stable boron isotopes at Ifremer (Plouzané, France) and reveals that neither cleaning protocol (oxidized vs. untreated), nor method of sample preparation (batch vs. column), nor injection system (d-DHIEN vs. ammonia addition) causes a significant difference in $\delta^{11}B_{CaCO3}$ composition of the samples. The batch method of boron extraction is preferred over the column chemistry method since the risk of B contamination is reduced in the batch
515 method due to shorter exposure to potential contaminants and smaller reagent volumes.

This newly established method for measuring stable boron isotopes at Ifremer was used to measure the $\delta^{11}B_{CaCO3}$ composition of six species of marine calcifiers that were all grown under equivalent seawater conditions. The coralline red alga *Neogoniolithion* sp. (35.89 ± 3.71 ‰; n = 3) exhibited the highest $\delta^{11}B_{CaCO3}$, followed by the temperate coral *O. arbuscula* (24.12 ± 0.19 ‰; n = 3), the tube of the serpulid worm *H. crucigera* (19.26 ± 0.16 ‰; n = 3), the tropical urchin
520 *E. tribuloides* (18.71 ± 0.26 ‰; n = 3), the temperate urchin *A. punctulata* (16.28 ± 0.86 ‰; n = 3), and the American oyster

© Author(s) 2017. CC-BY 3.0 License.

C. virginica (16.03 ‰; n = 1). The observed *ca.* 20 ‰ range in $\delta^{11}B_{CaCO3}$ composition of the investigated species constitutes the largest range in biogenic $\delta^{11}B_{CaCO3}$ reported to date.

Consideration of these extreme interspecific differences in $\delta^{11}B_{CaCO3}$ in the context of existing models of biomineralization for the investigated species, combined with published measurements of calcification site pH for some of the species, generally supports the assertion that most marine calcifiers precipitate their $CaCO_3$ from a discrete calcifying medium with a pH that is either greater than, equivalent to, or, for some species, less than external seawater pH. Furthermore, the observation that the different species' $\delta^{11}B_{CaCO3}$ and reconstructed calcification site pH generally varied inversely with their experimentally determined vulnerability to ocean acidification suggests that a species' relative resilience (or vulnerability) to OA may be influenced by their ability (or lack thereof) to maintain an elevated pH at their site of calcification. These observations contribute to the growing body of work that uses $\delta^{11}B_{CaCO3}$ as a tool to advance understanding of the mechanisms by which marine calcifiers build and maintain their shells and skeletons and, ultimately, how they will respond to anthropogenic ocean acidification.

© Author(s) 2017. CC-BY 3.0 License.

References

Addadi, L., Raz, S. and Weiner, S.: Taking Advantage of Disorder: Amorphous Calcium Carbonate and Its Roles in Biomineralization, Adv. Mater., 15(12), 959–970, doi:10.1002/adma.200300381, 2003.

Al-Ammar, A. S., Gupta, R. K. and Barnes, R. M.: Elimination of boron memory effect in inductively coupled plasma-mass spectrometry by ammonia gas injection into the spray chamber during analysis, Spectrochim. Acta Part B At. Spectrosc., 55(6), 629–635, doi:10.1016/S0584-8547(00)00197-X, 2000.

Al-Horani, F. A., Al-Moghrabi, S. M. and de Beer, D.: The mechanism of calcification and its relation to photosynthesis and respiration in the scleractinian coral Galaxea fascicularis, Mar. Biol., 142(3), 419–426, doi:10.1007/s00227-002-0981-8, 2003.

Allison, N. and Finch, A. A.: δ11B, Sr, Mg and B in a modern Porites coral: the relationship between calcification site pH and skeletal chemistry, Geochim. Cosmochim. Acta, 74(6), 1790–1800, doi:10.1016/j.gca.2009.12.030, 2010.

Ameye, L., Compère, P., Dille, J. and Dubois, P.: Ultrastructure and cytochemistry of the early calcification site and of its mineralization organic matrix in Paracentrotus lividus (Echinodermata: Echinoidea), Histochem. Cell Biol., 110(3), 285–294, doi:10.1007/s004180050290, 1998.

Anagnostou, E., Huang, K.-F., You, C.-F., Sikes, E. L. and Sherrell, R. M.: Evaluation of boron isotope ratio as a pH proxy in the deep sea coral Desmophyllum dianthus: Evidence of physiological pH adjustment, Earth Planet. Sci. Lett., 349–350, 251–260, doi:10.1016/j.epsl.2012.07.006, 2012.

Barker, S., Greaves, M. and Elderfield, H.: A study of cleaning procedures used for foraminiferal Mg/Ca paleothermometry, Geochemistry, Geophys. Geosystems, 4(9), 1–20, doi:10.1029/2003GC000559, 2003.

Bartoli, G., Hönisch, B. and Zeebe, R. E.: Atmospheric CO 2 decline during the Pliocene intensification of Northern Hemisphere glaciations, Paleoceanography, 26(4), doi:10.1029/2010PA002055, 2011.

Borowitzka, M. A. and Larkum, A. W. D.: Calcification in algae: Mechanisms and the role of metabolism, CRC. Crit. Rev. Plant Sci., 6(1), 1–45, doi:10.1080/07352688709382246, 1987.

Byrne, R. H., Yao, W., Klochko, K., Tossell, J. A. and Kaufman, A. J.: Experimental evaluation of the isotopic exchange equilibrium 10B(OH)3+11B(OH)4−=11B(OH)3+10B(OH)4− in aqueous solution, Deep Sea Res. Part I Oceanogr. Res. Pap., 53(4), 684–688, doi:10.1016/j.dsr.2006.01.005, 2006.

Cameron, J. N.: Post-Moult Calcification in the Blue Crab (Callinectes Sapidus): Relationships between Apparent Net H+ Excretion, Calcium and Bicarbonate, J. Exp. Biol., 119(1), 275 LP-285 [online] Available from: http://jeb.biologists.org/content/119/1/275.abstract, 1985.

Cohen, A. and Holcomb, M.: Why Corals Care About Ocean Acidification: Uncovering the Mechanism, Oceanography, 22(4), 118–127, doi:10.5670/oceanog.2009.102, 2009.

Cohen, A. L. and McConnaughey, T. A.: Geochemical Perspectives on Coral Mineralization, in Biomineralization, edited by P. M. Dove, J. J. De Yoreo, and S. Weiner, pp. 151–188, Mineralogical Society of America Geochemical Society., 2003.

Crenshaw, M. A.: The Inorganic Composition of Molluscan Extrapallial Fluid, Biol. Bull., 143(3), 506–512, doi:10.2307/1540180, 1972.

Cuif, J. P. and Dauphin, Y.: The Environment Recording Unit in coral skeletons – a synthesis of structural and chemical evidences for a biochemically driven, stepping-growth process in fibres, Biogeosciences, 2(1), 61–73, doi:10.5194/bg-2-61-2005, 2005.

Cusack, M., Kamenos, N. A., Rollion-Bard, C. and Tricot, G.: Red coralline algae assessed as marine pH proxies using 11B MAS NMR, Sci. Rep., 5, 8175, doi:10.1038/srep08175, 2015.

D'Olivo, J. P., McCulloch, M. T., Eggins, S. M. and Trotter, J.: Coral records of reef-water pH across the central Great Barrier Reef, Australia: assessing the influence of river runoff on inshore reefs, Biogeosciences, 12(4), 1223–1236, doi:10.5194/bg-12-1223-2015, 2015.

Dickson, A. G.: Thermodynamics of the dissociation of boric acid in synthetic seawater from 273.15 to 318.15 K, Deep Sea Res. Part A. Oceanogr. Res. Pap., 37(5), 755–766, doi:10.1016/0198-0149(90)90004-F, 1990.

© Author(s) 2017. CC-BY 3.0 License.

Dishon, G., Fisch, J., Horn, I., Kaczmarek, K., Bijma, J., Gruber, D. F., Nir, O., Popovich, Y. and Tchernov, D.: A novel paleo-bleaching proxy using boron isotopes and high-resolution laser ablation to reconstruct coral bleaching events, Biogeosciences, 12(19), 5677–5687, doi:10.5194/bg-12-5677-2015, 2015.

Dissard, D., Douville, E., Reynaud, S., Juillet-Leclerc, A., Montagna, P., Louvat, P. and McCulloch, M.: Light and temperature effects on δ11B and B / Ca ratios of the zooxanthellate coral Acropora sp.: results from culturing experiments, Biogeosciences, 9(11), 4589–4605, doi:10.5194/bg-9-4589-2012, 2012.

Doney, S. C., Fabry, V. J., Feely, R. A. and Kleypas, J. A.: Ocean Acidification: The Other CO 2Problem, Ann. Rev. Mar. Sci., 1(1), 169–192, doi:10.1146/annurev.marine.010908.163834, 2009.

Douville, E., Paterne, M., Cabioch, G., Louvat, P., Gaillardet, J., Juillet-Leclerc, A. and Ayliffe, L.: Abrupt sea surface pH change at the end of the Younger Dryas in the central sub-equatorial Pacific inferred from boron isotope abundance in corals (Porites), Biogeosciences, 7(8), 2445–2459, doi:10.5194/bg-7-2445-2010, 2010.

Fabry, V. J., Seibel, B. A., Feely, R. A. and Orr, J. C.: Impacts of ocean acidification on marine fauna and ecosystem processes, ICES J. Mar. Sci., 65(Dic), 414–432, 2008.

Farmer, J. R., Hönisch, B., Robinson, L. F. and Hill, T. M.: Effects of seawater-pH and biomineralization on the boron isotopic composition of deep-sea bamboo corals, Geochim. Cosmochim. Acta, 155, 86–106, doi:10.1016/j.gca.2015.01.018, 2015.

Foster, G. L.: Seawater pH, pCO2 and [CO2-3] variations in the Caribbean Sea over the last 130??kyr: A boron isotope and B/Ca study of planktic foraminifera, Earth Planet. Sci. Lett., 271(1–4), 254–266, doi:10.1016/j.epsl.2008.04.015, 2008.

Foster, G. L. and Sexton, P. F.: Enhanced carbon dioxide outgassing from the eastern equatorial Atlantic during the last glacial, Geology, 42(11), 1003–1006, doi:10.1130/G35806.1, 2014.

Foster, G. L., Pogge Von Strandmann, P. A. E. and Rae, J. W. B.: Boron and magnesium isotopic composition of seawater, Geochemistry, Geophys. Geosystems, 11(8), 1–10, doi:10.1029/2010GC003201, 2010.

Foster, G. L., Lear, C. H. and Rae, J. W. B.: The evolution of pCO2, ice volume and climate during the middle Miocene, Earth Planet. Sci. Lett., 341–344, 243–254, doi:10.1016/j.epsl.2012.06.007, 2012.

Foster, G. L., Hönisch, B., Paris, G., Dwyer, G. S., Rae, J. W. B., Elliott, T., Gaillardet, J., Hemming, N. G., Louvat, P. and Vengosh, A.: Interlaboratory comparison of boron isotope analyses of boric acid, seawater and marine CaCO3 by MC-ICPMS and NTIMS, Chem. Geol., 358, 1–14, doi:10.1016/j.chemgeo.2013.08.027, 2013.

Gaetani, G. A. and Cohen, A. L.: Element partitioning during precipitation of aragonite from seawater: A framework for understanding paleoproxies, Geochim. Cosmochim. Acta, 70(18), 4617–4634, doi:10.1016/j.gca.2006.07.008, 2006.

Gaillardet, J. and Allègre, C. J.: Boron isotopic compositions of corals: Seawater or diagenesis record?, Earth Planet. Sci. Lett., 136(3–4), 665–676, doi:10.1016/0012-821X(95)00180-K, 1995.

Goldberg, W. M.: Desmocytes in the calicoblastic epithelium of the stony coral Mycetophyllia reesi and their attachment to the skeleton, Tissue Cell, 33(4), 388–394, doi:10.1054/tice.2001.0192, 2001.

Hedley, R. H.: Studies of Serpulid Tube Formation. I. The secretion of the Calcareous and Organic Components of the Tube by Pomatoceros triqueter., Quaterly Journval Microsc. Sci., 97(September), 411–419, 1956.

Heinemann, A., Fietzke, J., Melzner, F., Böhm, F., Thomsen, J., Garbe-Schnberg, D. and Eisenhauer, A.: Conditions of Mytilus edulis extracellular body fluids and shell composition in a pH-treatment experiment: Acid-base status, trace elements and δ^{11}B, Geochemistry, Geophys. Geosystems, 13(1), doi:10.1029/2011GC003790, 2012.

Hemming, N. G. and Hanson, G. N.: Boron isotopic composition and concentration in modern marine carbonates, Geochim. Cosmochim. Acta, 56(1), 537–543, doi:10.1016/0016-7037(92)90151-8, 1992.

Hemming, N. G. and Hönisch, B.: Chapter Seventeen Boron Isotopes in Marine Carbonate Sediments and the pH of the Ocean, in Developments in Marine Geology, vol. 1, pp. 717–734., 2007.

Hemming, N. G., Guilderson, T. P. and Fairbanks, R. G.: Seasonal variations in the boron isotopic composition of coral: A productivity signal?, Global Biogeochem. Cycles, 12(4), 581–586, doi:10.1029/98GB02337, 1998.

Holcomb, M., McCorkle, D. C. and Cohen, A. L.: Long-term effects of nutrient and CO2 enrichment on the temperate coral

© Author(s) 2017. CC-BY 3.0 License.

Astrangia poculata (Ellis and Solander, 1786), J. Exp. Mar. Bio. Ecol., 386(1–2), 27–33, doi:10.1016/j.jembe.2010.02.007, 2010.

Holcomb, M., Venn, A. A., Tambutté, E., Tambutté, S., Allemand, D., Trotter, J. and McCulloch, M.: Coral calcifying fluid pH dictates response to ocean acidification, Sci. Rep., 4, doi:10.1038/srep05207, 2014.

Hönisch, B. and Hemming, N. G.: Ground-truthing the boron isotope-paleo-pH proxy in planktonic foraminifera shells: Partial dissolution and shell size effects, Paleoceanography, 19(4), n/a-n/a, doi:10.1029/2004PA001026, 2004.

Hönisch, B. and Hemming, N. G.: Surface ocean pH response to variations in pCO2 through two full glacial cycles, Earth Planet. Sci. Lett., 236(1–2), 305–314, doi:10.1016/j.epsl.2005.04.027, 2005.

Hönisch, B., Hemming, N. G., Grottoli, A. G., Amat, A., Hanson, G. N. and Bijma, J.: Assessing scleractinian corals as recorders for paleo-pH: Empirical calibration and vital effects, Geochim. Cosmochim. Acta, 68(18), 3675–3685, doi:10.1016/j.gca.2004.03.002, 2004.

Hönisch, B., Hemming, N. G., Archer, D., Siddall, M. and McManus, J. F.: Atmospheric carbon dioxide concentration across the mid-Pleistocene transition., Science, 324(5934), 1551–4, doi:10.1126/science.1171477, 2009.

IPCC: Climate Change 2013 - The Physical Science Basis, edited by Intergovernmental Panel on Climate Change, Cambridge University Press, Cambridge., 2014.

Kaczmarek, K., Langer, G., Nehrke, G., Horn, I., Misra, S., Janse, M. and Bijma, J.: Boron incorporation in the foraminifer Amphistegina lessonii under a decoupled carbonate chemistry, Biogeosciences, 12(6), 1753–1763, doi:10.5194/bg-12-1753-2015, 2015.

Kakihana, H., Kotaka, M., Satoh, S., Nomura, M. and Okamoto, M.: Fundamental Studies on the Ion-Exchange Separation of Boron Isotopes, Bull. Chem. Soc. Jpn., 50(1), 158–163, doi:10.1246/bcsj.50.158, 1977.

Kasemann, S. A., Schmidt, D. N., Bijma, J. and Foster, G. L.: In situ boron isotope analysis in marine carbonates and its application for foraminifera and palaeo-pH, Chem. Geol., 260(1–2), 138–147, doi:10.1016/j.chemgeo.2008.12.015, 2009.

Kiss, E.: Ion-exchange separation and spectrophotometric determination of boron in geological materials, Anal. Chim. Acta, 211, 243–256, doi:10.1016/S0003-2670(00)83684-3, 1988.

Kleypas, J. A., Feely, R. A., Fabry, V. J., Langdon, C., Sabine, C. L. and Robbins, L. L.: Impacts of ocean acidification on coral reefs and other marine calcifiers. A guide for future research., 2006.

Klochko, K., Kaufman, A. J., Yao, W., Byrne, R. H. and Tossell, J. A.: Experimental measurement of boron isotope fractionation in seawater, Earth Planet. Sci. Lett., 248(1–2), 276–285, doi:10.1016/j.epsl.2006.05.034, 2006.

Klochko, K., Cody, G. D., Tossell, J. A., Dera, P. and Kaufman, A. J.: Re-evaluating boron speciation in biogenic calcite and aragonite using 11B MAS NMR, Geochim. Cosmochim. Acta, 73(7), 1890–1900, doi:10.1016/j.gca.2009.01.002, 2009.

Krief, S., Hendy, E. J., Fine, M., Yam, R., Meibom, A., Foster, G. L. and Shemesh, A.: Physiological and isotopic responses of scleractinian corals to ocean acidification, Geochim. Cosmochim. Acta, 74(17), 4988–5001, doi:10.1016/j.gca.2010.05.023, 2010.

Kroeker, K. J., Kordas, R. L., Crim, R. N. and Singh, G. G.: Meta-analysis reveals negative yet variable effects of ocean acidification on marine organisms, Ecol. Lett., 13(11), 1419–1434, doi:10.1111/j.1461-0248.2010.01518.x, 2010.

Kroeker, K. J., Kordas, R. L., Crim, R., Hendriks, I. E., Ramajo, L., Singh, G. S., Duarte, C. M. and Gattuso, J. P.: Impacts of ocean acidification on marine organisms: Quantifying sensitivities and interaction with warming, Glob. Chang. Biol., 19(6), 1884–1896, doi:10.1111/gcb.12179, 2013.

Kubota, K., Yokoyama, Y., Ishikawa, T., Obrochta, S. and Suzuki, A.: Larger CO2 source at the equatorial Pacific during the last deglaciation., Sci. Rep., 4, 5261, doi:10.1038/srep05261, 2014.

Langdon, C.: Review of experimental evidence for effects of CO2 on calcification of reef builders., in Proc. 9th Int. Coral Reef Sym, pp. 1–8. [online] Available from: http://people.uncw.edu/szmanta/2006 pdfs/20 Global warming issues/Langdon 9I CRSProceedings CO2 calcification.pdf, 2002.

Lee, D. and Carpenter, S. J.: Isotopic disequilibrium in marine calcareous algae, Chem. Geol., 172(3–4), 307–329, doi:10.1016/S0009-2541(00)00258-8, 2001.

© Author(s) 2017. CC-BY 3.0 License.

Lemarchand, D., Gaillardet, J., Lewin, É. and Allègre, C. J.: The influence of rivers on marine boron isotopes and implications for reconstructing past ocean pH, Nature, 408(6815), 951–954, doi:10.1038/35050058, 2000.

Lemarchand, D., Gaillardet, J., Göpel, C. and Manhès, G.: An optimized procedure for boron separation and mass spectrometry analysis for river samples, Chem. Geol., 182(2–4), 323–334, doi:10.1016/S0009-2541(01)00329-1, 2002.

Littlewood, D. T. J. and Young, R. E.: The effect of air-gaping behaviour on extrapallial fluid pH in the tropical oyster Crassostrea rhizophorae, Comp. Biochem. Physiol. Part A Physiol., 107(1), 1–6, doi:10.1016/0300-9629(94)90264-X, 1994.

Liu, Y. and Tossell, J. A.: Ab initio molecular orbital calculations for boron isotope fractionations on boric acids and borates, Geochim. Cosmochim. Acta, 69(16), 3995–4006, doi:10.1016/j.gca.2005.04.009, 2005.

Liu, Y., Liu, W., Peng, Z., Xiao, Y., Wei, G., Sun, W., He, J., Liu, G. and Chou, C. L.: Instability of seawater pH in the South China Sea during the mid-late Holocene: Evidence from boron isotopic composition of corals, Geochim. Cosmochim. Acta, 73(5), 1264–1272, doi:10.1016/j.gca.2008.11.034, 2009.

Louvat, P., Bouchez, J. and Paris, G.: MC-ICP-MS Isotope Measurements with Direct Injection Nebulisation (d-DIHEN): Optimisation and Application to Boron in Seawater and Carbonate Samples, Geostand. Geoanalytical Res., 35(1), 75–88, doi:10.1111/j.1751-908X.2010.00057.x, 2011.

Louvat, P., Moureau, J., Paris, G., Bouchez, J., Noireaux, J. and Gaillardet, J. J. J.: A fully automated direct injection nebulizer (d-DIHEN) for MC-ICP-MS isotope analysis: application to boron isotope ratio measurements, J. Anal. At. Spectrom., 29(9), doi:10.1039/C4JA00098F, 2014.

Marie, B., Joubert, C., Tayale, A., Zanella-Cleon, I., Belliard, C., Piquemal, D., Cochennec-Laureau, N., Marin, F., Gueguen, Y. and Montagnani, C.: Different secretory repertoires control the biomineralization processes of prism and nacre deposition of the pearl oyster shell, Proc. Natl. Acad. Sci., 109(51), 20986–20991, doi:10.1073/pnas.1210552109, 2012.

Martínez-Botí, M. a., Foster, G. L., Chalk, T. B., Rohling, E. J., Sexton, P. F., Lunt, D. J., Pancost, R. D., Badger, M. P. S. and Schmidt, D. N.: Plio-Pleistocene climate sensitivity evaluated using high-resolution CO2 records, Nature, 518(7537), 49–54, doi:10.1038/nature14145, 2015a.

Martínez-Botí, M. A., Marino, G., Foster, G. L., Ziveri, P., Henehan, M. J., Rae, J. W. B., Mortyn, P. G. and Vance, D.: Boron isotope evidence for oceanic carbon dioxide leakage during the last deglaciation, Nature, 518, 219–222, doi:10.1038/nature14155, 2015b.

McConnaughey, T.: 13C and 18O isotopic disequilibrium in biological carbonates: I. Patterns, Geochim. Cosmochim. Acta, 53(1), 151–162, doi:10.1016/0016-7037(89)90282-2, 1989.

McConnaughey, T. A. and Falk, R. H.: Calcium-Proton Exchange during Algal Calcification, Biol. Bull., 180(1), 185–195, doi:10.2307/1542440, 1991.

McConnaughey, T. A. and Whelan, J. F.: Calcification generates protons for nutrient and bicarbonate uptake, Earth-Science Rev., 42(1–2), 95–117, doi:10.1016/S0012-8252(96)00036-0, 1997.

McCulloch, M., Falter, J., Trotter, J. and Montagna, P.: Coral resilience to ocean acidification and global warming through pH up-regulation, Nat. Clim. Chang., 2(8), 623–627, doi:10.1038/nclimate1473, 2012.

McCulloch, M. T., Holcomb, M., Rankenburg, K. and Trotter, J. A.: Rapid, high-precision measurements of boron isotopic compositions in marine carbonates, Rapid Commun. Mass Spectrom., 28(24), 2704–2712, doi:10.1002/rcm.7065, 2014.

Meibom, A., Cuif, J. P., Houlbreque, F., Mostefaoui, S., Dauphin, Y., Meibom, K. L. and Dunbar, R.: Compositional variations at ultra-structure length scales in coral skeleton, Geochim. Cosmochim. Acta, 72(6), 1555–1569, doi:10.1016/j.gca.2008.01.009, 2008.

Michaelidis, B., Haas, D. and Grieshaber, M. K.: Extracellular and Intracellular Acid-Base Status with Regard to the Energy Metabolism in the Oyster Crassostrea gigas during Exposure to Air, Physiol. Biochem. Zool., 78(3), 373–383, doi:10.1086/430223, 2005.

Montagna, P., McCulloch, M., Mazzoli, C., Silenzi, S. and Odorico, R.: The non-tropical coral Cladocora caespitosa as the new climate archive for the Mediterranean: high-resolution (~weekly) trace element systematics, Quat. Sci. Rev., 26(3–4), 441–462, doi:10.1016/j.quascirev.2006.09.008, 2007.

Mount, A. S., Wheeler, a P., Paradkar, R. P. and Snider, D.: Hemocyte-mediated shell mineralization in the eastern oyster.,

© Author(s) 2017. CC-BY 3.0 License.

Science, 304(5668), 297–300, doi:10.1126/science.1090506, 2004.

Ni, Y., Foster, G. L., Bailey, T., Elliott, T., Schmidt, D. N., Pearson, P., Haley, B. and Coath, C.: A core top assessment of proxies for the ocean carbonate system in surface-dwelling foraminifers, Paleoceanography, 22(3), doi:10.1029/2006PA001337, 2007.

Nir, O., Vengosh, A., Harkness, J. S., Dwyer, G. S. and Lahav, O.: Direct measurement of the boron isotope fractionation factor: Reducing the uncertainty in reconstructing ocean paleo-pH, Earth Planet. Sci. Lett., 414, 1–5, doi:10.1016/j.epsl.2015.01.006, 2015.

Noireaux, J., Mavromatis, V., Gaillardet, J., Schott, J., Montouillout, V., Louvat, P., Rollion-Bard, C. and Neuville, D. R.: Crystallographic control on the boron isotope paleo-pH proxy, Earth Planet. Sci. Lett., 430(November 2015), 398–407, doi:10.1016/j.epsl.2015.07.063, 2015.

Pagani, M., Lemarchand, D., Spivack, A. and Gaillardet, J.: A critical evaluation of the boron isotope-pH proxy: The accuracy of ancient ocean pH estimates, Geochim. Cosmochim. Acta, 69(4), 953–961, doi:10.1016/j.gca.2004.07.029, 2005.

Palmer, M. R.: Reconstructing Past Ocean pH-Depth Profiles, Science (80-.)., 282(5393), 1468–1471, doi:10.1126/science.282.5393.1468, 1998.

Palmer, M. R., Spivack, A. J. and Edmond, J. M.: Temperature and pH controls over isotopic fractionation during absorption of boron marine clay., Geochim. Cosmochim. Acta., 51(9), 2319–2323, doi:http://dx.doi.org/10.1016/0016-7037(87)90285-7, 1987.

Palmer, M. R., Brummer, G. J., Cooper, M. J., Elderfield, H., Greaves, M. J., Reichart, G. J., Schouten, S. and Yu, J. M.: Multi-proxy reconstruction of surface water pCO2 in the northern Arabian Sea since 29ka, Earth Planet. Sci. Lett., 295(1–2), 49–57, doi:10.1016/j.epsl.2010.03.023, 2010.

Pearson, P. and Palmer, M.: Middle eocene seawater pH and atmospheric carbon dioxide concentrations, Science, 284(5421), 1824–6 [online] Available from: http://www.ncbi.nlm.nih.gov/pubmed/10364552, 1999.

Pearson, P. N. and Palmer, M. R.: Atmospheric carbon dioxide concentrations over the past 60 million years , Nature, 406(6797), 695–699 [online] Available from: http://dx.doi.org/10.1038/35021000, 2000.

Pearson, P. N., Foster, G. L. and Wade, B. S.: Atmospheric carbon dioxide through the Eocene–Oligocene climate transition, Nature, 461(7267), 1110–1113 [online] Available from: http://dx.doi.org/10.1038/nature08447, 2009.

Penman, D. and Hönisch, B.: Rapid and sustained surface ocean acidification during the Paleocene-Eocene Thermal Maximum, Paleoceanography, 1–13, doi:10.1002/2014PA002621.Received, 2014.

Rae, J. W. B., Foster, G. L., Schmidt, D. N. and Elliott, T.: Boron isotopes and B/Ca in benthic foraminifera: Proxies for the deep ocean carbonate system, Earth Planet. Sci. Lett., 302(3–4), 403–413, doi:10.1016/j.epsl.2010.12.034, 2011.

Rae, J. W. B., Sarnthein, M., Foster, G. L., Ridgwell, A., Grootes, P. M. and Elliott, T.: Deep water formation in the North Pacific and deglacial CO 2 rise, Paleoceanography, 29(6), 645–667, doi:10.1002/2013PA002570, 2014.

Reynaud, S., Hemming, N. G., Juillet-Leclerc, A. and Gattuso, J. P.: Effect of pCO2 and temperature on the boron isotopic composition of the zooxanthellate coral Acropora sp., Coral Reefs, 23(4), 539–546, doi:10.1007/s00338-004-0399-5, 2004.

Ries, J. B.: A physicochemical framework for interpreting the biological calcification response to CO2-induced ocean acidification, Geochim. Cosmochim. Acta, 75(14), 4053–4064, doi:10.1016/j.gca.2011.04.025, 2011a.

Ries, J. B.: Skeletal mineralogy in a high-CO2 world, J. Exp. Mar. Bio. Ecol., 403(1–2), 54–64, doi:10.1016/j.jembe.2011.04.006, 2011b.

Ries, J. B., Cohen, A. L. and McCorkle, D. C.: Marine calcifiers exhibit mixed responses to CO2-induced ocean acidification, Geology, 37(12), 1131–1134, doi:10.1130/G30210A.1, 2009.

Rink, S., Kühl, M., Bijma, J. and Spero, H. J.: Microsensor studies of photosynthesis and respiration in the symbiotic foraminifer Orbulina universa, Mar. Biol., 131(4), 583–595, doi:10.1007/s002270050350, 1998.

Rollion-Bard, C. and Erez, J.: Intra-shell boron isotope ratios in the symbiont-bearing benthic foraminiferan Amphistegina lobifera: Implications for ??11B vital effects and paleo-pH reconstructions, Geochim. Cosmochim. Acta, 74(5), 1530–1536, doi:10.1016/j.gca.2009.11.017, 2010.

© Author(s) 2017. CC-BY 3.0 License.

760 Rollion-Bard, C., Chaussidon, M. and France-Lanord, C.: Biological control of internal pH in scleractinian corals: Implications on paleo-pH and paleo-temperature reconstructions, Comptes Rendus - Geosci., 343(6), 397–405, doi:10.1016/j.crte.2011.05.003, 2011a.

Rollion-Bard, C., Blamart, D., Trebosc, J., Tricot, G., Mussi, A. and Cuif, J. P.: Boron isotopes as pH proxy: A new look at boron speciation in deep-sea corals using 11B MAS NMR and EELS, Geochim. Cosmochim. Acta, 75(4), 1003–1012, 765 doi:10.1016/j.gca.2010.11.023, 2011b.

Rustad, J. R. and Bylaska, E. J.: Ab Initio Calculation of Isotopic Fractionation in B(OH)3 (aq) and BOH4- (aq), J. Am. Chem. Soc., 129(8), 2222–2223, doi:10.1021/ja0683335, 2007.

Saenger, C., Wang, Z., Gaetani, G., Cohen, A. and Lough, J. M.: The influence of temperature and vital effects on magnesium isotope variability in Porites and Astrangia corals, Chem. Geol., 360–361, 105–117, 770 doi:10.1016/j.chemgeo.2013.09.017, 2013.

Sanyal, A., Hemming, N. G., Hanson, G. N. and Broecker, W. S.: Evidence for a higher pH in the glacial ocean from boron isotopes in foraminifera, Nature, 373(6511), 234–236, doi:10.1038/373234a0, 1995.

Sanyal, A., Hemming, N. G., Broecker, W. S. and Hanson, G. N.: Changes in p H in the eastern equatorial Pacific across stage 5-6 boundary based on boron isotopes in foraminifera, Global Biogeochem. Cycles, 11(1), 125–133, 775 doi:10.1029/97GB00223, 1997.

Sanyal, A., Nugent, M., Reeder, R. J. and Bijma, J.: Seawater pH control on the boron isotopic composition of calcite: evidence from inorganic calcite precipitation experiments, Geochim. Cosmochim. Acta, 64(9), 1551–1555, doi:10.1016/S0016-7037(99)00437-8, 2000.

Sanyal, A., Bijma, J., Spero, H. and Lea, D. W.: Empirical relationship between pH and the boron isotopic composition of 780 Globigerinoides sacculifer : Implications for the boron isotope paleo-pH proxy, Paleoceanography, 16(5), 515–519, doi:10.1029/2000PA000547, 2001.

Schoepf, V., McCulloch, M. T., Warner, M. E., Levas, S. J., Matsui, Y., Aschaffenburg, M. D. and Grottoli, A. G.: Short-Term Coral Bleaching Is Not Recorded by Skeletal Boron Isotopes, edited by C. R. Voolstra, PLoS One, 9(11), e112011, doi:10.1371/journal.pone.0112011, 2014.

785 Short, J. A., Pedersen, O. and Kendrick, G. A.: Turf algal epiphytes metabolically induce local pH increase, with implications for underlying coralline algae under ocean acidification, Estuar. Coast. Shelf Sci., 164, 463–470, doi:10.1016/j.ecss.2015.08.006, 2015.

Simkiss, K. and Wilbur, K. M.: Biomineralization: Cell Biology and Miberal Deposition, Academic Press, San Diego., 1989.

Spivak, A. J. (Scripps), You, C.-F. and Smith, J.: Spivack et al 1993.pdf, Nature, 363(may 13), 149–151, 1993.

790 Stumpp, M., Hu, M. Y., Melzner, F., Gutowska, M. A. and Dorey, N.: Acidified seawater impacts sea urchin larvae pH regulatory systems relevant for calcification, , doi:10.1073/pnas.1209174109/-/DCSupplemental.www.pnas.org/cgi/doi/10.1073/pnas.1209174109, 2012.

Tambutté, E., Allemand, D., Zoccola, D., Meibom, A., Lotto, S., Caminiti, N. and Tambutté, S.: Observations of the tissue-skeleton interface in the scleractinian coral Stylophora pistillata, Coral Reefs, 26(3), 517–529, doi:10.1007/s00338-007-795 0263-5, 2007.

Trotter, J., Montagna, P., McCulloch, M., Silenzi, S., Reynaud, S., Mortimer, G., Martin, S., Ferrier-Pagès, C., Gattuso, J. P. and Rodolfo-Metalpa, R.: Quantifying the pH "vital effect" in the temperate zooxanthellate coral Cladocora caespitosa: Validation of the boron seawater pH proxy, Earth Planet. Sci. Lett., 303(3–4), 163–173, doi:10.1016/j.epsl.2011.01.030, 2011.

800 Vengosh, A., Kolodny, Y., Starinsky, A., Chivas, A. R. and McCulloch, M. T.: Coprecipitation and isotopic fractionation of boron in modern biogenic carbonates, Geochim. Cosmochim. Acta, 55(10), 2901–2910, doi:10.1016/0016-7037(91)90455-E, 1991.

Venn, A., Tambutté, E., Holcomb, M., Allemand, D. and Tambutté, S.: Live tissue imaging shows reef corals elevate pH under their calcifying tissue relative to seawater, PLoS One, 6(5), doi:10.1371/journal.pone.0020013, 2011.

805 Venn, A. A., Tambutté, E., Lotto, S., Zoccola, D., Allemand, D. and Tambutté, S.: Imaging intracellular pH in a reef coral and symbiotic anemone., Proc. Natl. Acad. Sci. U. S. A., 106(39), 16574–9, doi:10.1073/pnas.0902894106, 2009.

© Author(s) 2017. CC-BY 3.0 License.

Venn, A. A., Tambutté, E., Holcomb, M., Laurent, J., Allemand, D. and Tambutté, S.: Impact of seawater acidification on pH at the tissue-skeleton interface and calcification in reef corals., Proc. Natl. Acad. Sci. U. S. A., 110(5), 1634–9, doi:10.1073/pnas.1216153110, 2013.

Wall, M., Fietzke, J., Schmidt, G. M., Fink, A., Hofmann, L. C., de Beer, D. and Fabricius, K. E.: Internal pH regulation facilitates in situ long-term acclimation of massive corals to end-of-century carbon dioxide conditions, Sci. Rep., 6, 30688 [online] Available from: http://dx.doi.org/10.1038/srep30688, 2016.

Wang, B.-S., You, C.-F., Huang, K.-F., Wu, S.-F., Aggarwal, S. K., Chung, C.-H. and Lin, P.-Y.: Direct separation of boron from Na-and Ca-rich matrices by sublimation for stable isotope measurement by MC-ICP-MS, Talanta, 82(4), 1378–1384, 2010.

Wei, G., McCulloch, M. T., Mortimer, G., Deng, W. and Xie, L.: Evidence for ocean acidification in the Great Barrier Reef of Australia, Geochim. Cosmochim. Acta, 73(8), 2332–2346, doi:10.1016/j.gca.2009.02.009, 2009.

Weiner, S., Traub, W. and Parker, S. B.: Macromolecules in Mollusc Shells and Their Functions in Biomineralization [and Discussion], Philos. Trans. R. Soc. B Biol. Sci., 304(1121), 425–434, doi:10.1098/rstb.1984.0036, 1984.

Wheeler, A.: Mechanisms of molluscan shell formation., in Calcification in biolgical systems, edited by E. Bonucci, pp. 179–216, CRC Press., 1992.

Wilbur, K. and Saleuddin, A.: Shell formation, in The Mollusca, edited by K. Wilbur and A. Saleuddin, pp. 235–287, Academic., 1983.

Xiao, J., Jin, Z. D., Xiao, Y. K. and He, M. Y.: Controlling factors of the δ11B-pH proxy and its research direction, Environ. Earth Sci., 71(4), 1641–1650, doi:10.1007/s12665-013-2568-8, 2014.

Yu, J., Foster, G. L., Elderfield, H., Broecker, W. S. and Clark, E.: An evaluation of benthic foraminiferal B/Ca and δ11B for deep ocean carbonate ion and pH reconstructions, Earth Planet. Sci. Lett., 293(1–2), 114–120, doi:10.1016/j.epsl.2010.02.029, 2010.

Yu, J., Thornalley, D. J. R., Rae, J. W. B. and McCave, N. I.: Calibration and application of B/Ca, Cd/Ca, and δ11B in Neogloboquadrina pachyderma (sinistral) to constrain CO2 uptake in the subpolar North Atlantic during the last deglaciation, Paleoceanography, 28(2), 237–252, doi:10.1002/palo.20024, 2013.

Zeebe, R. E.: Stable boron isotope fractionation between dissolved B(OH)3 and B(OH)4-, Geochim. Cosmochim. Acta, 69(11), 2753–2766, doi:10.1016/j.gca.2004.12.011, 2005.

Zeebe, R. E. and Sanyal, A.: Comparison of two potential strategies of planktonic foraminifera for house building: Mg2+ or H+ removal?, Geochim. Cosmochim. Acta, 66(7), 1159–1169, doi:10.1016/S0016-7037(01)00852-3, 2002.

Zinke, J., Rountrey, A., Feng, M., Xie, S.-P., Dissard, D., Rankenburg, K., Lough, J. M. and McCulloch, M. T.: Corals record long-term Leeuwin current variability including Ningaloo Niño/Niña since 1795, Nat. Commun., 5, doi:10.1038/ncomms4607, 2014.

Biogeosciences Discuss., doi:10.5194/bg-2017-154, 2017
Manuscript under review for journal Biogeosciences
Discussion started: 15 May 2017
© Author(s) 2017. CC-BY 3.0 License.

Tables

Table 1. Protocol used to evaluate the column chemistry method of boron extraction. Three volumes of resin (60, 250 and 500 µL) were evaluated.

Step	mg resin	15	62.5	125
1	Resin (uL)	60	250	500
2	MQ H2O at pH 7 (mL)	5	5	5
3	0.5 N HNO3 (mL)	2.5	2.5	5
4	MQ H2O at pH 7 (mL) x3	2.5	2.5	5
5	Check pH			
6	Sample Load (ng)	536	536	536
7	MQ H2O at pH 7 (mL) x3	1	1	2
10	Check pH			
11	0.05N HNO3 (mL)	0.5	0.5	0.5
22	MQ H2O at pH 7 (mL)	2	2	2

Table 2. Mass spectrometer operating conditions.

	d-DIHEN	**Ammonia Addition**
Injection system	Demountable Direct Injection Nebulizer	PFA teflon spray chamber with ESI PFA teflon 50 µL min^{-1} nebuliser
Sample Gas Flow Rate	0.3 L min-	1.1 L min^{-1}
Running Concentrations	B = 50 ppb	B = 30 – 50 ppb (evaluated 30, 65, 130 ppb)
Sensitivity	35 V ppm^{-1}, total B	20 V ppm^{-1}, total B
Blank Level	< 0.5 % of ^{11}B signal after 30s in 2 % HNO_3, 0.1 % after 120s	< 5 % of ^{11}B signal after 30s in 0.05% HNO_3, 3% after 120s
Resolution	Low	Low
Forward Power	1200 W	1200 W
Accelerating Voltage	10 kV	10 kV
Plasma Mode	Wet Plasma	Wet Plasma
Cool Gas Flow Rate	16 L min^{-1}	16 L min^{-1}
Auxiliary Gas Flow Rate	0.9 L min^{-1}	0.9 L min^{-1}
Sampler Cone	Standard Ni cone	Standard Ni cone
Skimmer Cone	X Ni cone	X Ni cone
Interferences	$^{40}Ar^{++++}$ $^{20}Ne^{++}$ resolved	$^{40}Ar^{++++}$ $^{20}Ne^{++}$ resolved
Accuracy	0.2 ‰, 2sd, n = 6	0.2 ‰, 2sd, n = 6
Acquisition	30 x 4s	30 x 4s
Baselines	Counting times of 20 s	Counting times of 20 s

Biogeosciences Discuss., doi:10.5194/bg-2017-154, 2017
Manuscript under review for journal Biogeosciences
Discussion started: 15 May 2017
© Author(s) 2017. CC-BY 3.0 License.

Table 3. Boron isotope composition ($\delta^{11}B$; ‰) of all species evaluated, including international carbonate standards JCP-1 (*Porites* sp.) and JCt-1 (Hard clam). Data are presented as average of *n* analyses and the precision is reported as 2 standard deviations (2SD). The cleaning protocol (Oxidised – 'Ox'/Uncleaned – 'U'), separation method ('column'/'batch'), and injection method ('NH_3'/'d-DIHEN') are presented for comparison.

855

Sample type	Name	$\delta^{11}B$	(2SD)	*n*	Cleaning	Separation	Injection
Hard clam	JCt-1	17.50	0.60	12	Ox	batch	d-DIHEN
Hard clam	JCt-1	16.90	0.30	6	Ox	batch	NH_3
Hard clam	JCt-1	16.34	0.64	2	Ox	column	NH_3
Hard clam	JCt-1	16.24	0.42	2	U	batch	NH_3
Porites coral	JCp-1	24.52	0.34	6	Ox	column	NH_3
Porites coral	JCp-1	24.30	0.16	10	Ox	batch	d-DIHEN
Porites coral	JCp-1	24.65	0.60	6	Ox	batch	NH_3
Porites coral	JCp-1	24.44	0.56	6	U	column	NH_3
Porites coral	JCp-1	24.41	0.30	6	U	batch	NH_3
Porites coral	JCp-1	24.36	0.51	2	Ox	column	NH_3
Porites coral	JCp-1	24.24	0.38	2	Ox	batch	NH_3
Porites coral	NEP-1	26.56	0.34	2	U	batch	NH_3
Porites coral	NEP-1	25.51	0.38	2	Ox	column	NH_3
Porites coral	NEP-1	25.34	0.78	2	Ox	batch	NH_3
Porites coral	NEP-1	25.52	0.46	2	U	column	NH_3
Porites coral	NEP-1	25.92	0.12	2	U	batch	NH_3
Porites coral	NEP-1	25.96	0.30	2	Ox	batch	NH_3
Temperate coral	OCU-9	24.04	na	1	Ox	batch	NH_3
Temperate coral	OCU-10	23.98	na	1	Ox	batch	NH_3
Temperate coral	OCU-11	24.34	na	1	Ox	batch	NH_3
Coralline alga	JR-19	39.94	0.12	2	Ox	batch	NH_3
Coralline alga	JR-20	32.65	0.46	2	Ox	batch	NH_3
Coralline alga	JR-20	32.68	0.22	2	Ox	column	NH_3
Coralline alga	JR-21	35.07	na	1	Ox	batch	NH_3
Tropical urchin	JR-56	19.00	0.36	2	Ox	batch	NH_3
Tropical urchin	JR-57	18.64	0.11	2	Ox	batch	NH_3
Tropical urchin	JR-58	18.49	0.09	2	Ox	batch	NH_3
Temperate urchin	JR-64	14.96	0.10	2	Ox	column	NH_3
Temperate urchin	JR-64	17.60	0.80	2	Ox	batch	d-DIHEN
Temperate urchin	JR-65	17.11	1.10	2	Ox	batch	NH_3
Temperate urchin	JR-66	15.43	0.11	2	Ox	batch	NH_3
Serpulid worm tube	JR-1	19.44	na	1	Ox	batch	NH_3
Serpulid worm tube	JR-2	19.13	na	1	Ox	batch	NH_3
Serpulid worm tube	JR-3	19.21	na	1	Ox	batch	NH_3
American oyster	JR125	16.18	0.16	2	Ox	column	NH_3
American oyster	JR125	15.90	0.60	2	Ox	batch	d-DIHEN
American oyster	JR125	16.00	0.32	2	U	batch	NH_3

Biogeosciences Discuss., doi:10.5194/bg-2017-154, 2017
Manuscript under review for journal Biogeosciences
Discussion started: 15 May 2017
© Author(s) 2017. CC-BY 3.0 License.

Table 4. Summary of the average $\delta^{11}B$ (‰), standard deviation (SD) of $\delta^{11}B$ for each species (‰), calculated pH at calcification site (pH_{CS}), pH of the seawater (pH_{SW}) during the experimental conditions, and difference between pH_{CS} and pH_{SW} (ΔpH). The Ocean Acidification Response (OA Response) and mineralogy were previously described by Ries et al. (Ries et al., 2009). The abbreviations HMC and LMC describe high-Mg calcite and low-Mg calcite. Typically, 3 biological replicates of each species were measured. 'NA' = not available, only one biological replicate analysed.

Sample Type	Scientific Name	$\delta^{11}B$ (SD)	pH_{CS}	pH_{SW}	ΔpH	OA Response	Mineralogy
Coralline alga	*Neogoniolithion* sp.	**35.89** (3.71)	9.4	8.1	1.3	Parabolic	HMC
Temperate coral	*Oculina arbuscula*	**24.12** (0.19)	8.5	8.1	0.4	Threshold	Aragonite
Tropical urchin	*Eucidaris tribuloides*	**18.71** (0.26)	8.1	8.0	0.1	Threshold	HMC
Serpulid worm	*Hydroides crucigera*	**19.26** (0.16)	8.2	8.1	0.1	Negative	Aragonite+HMC
Temperate urchin	*Arbacia punctulata*	**16.28** (0.86)	7.9	8.0	-0.1	Parabolic	HMC
American oyster	*Crassostrea virginica*	**16.03** (NA)	7.9	8.2	-0.3	Negative	LMC

Biogeosciences Discuss., doi:10.5194/bg-2017-154, 2017
Manuscript under review for journal Biogeosciences
Discussion started: 15 May 2017
© Author(s) 2017. CC-BY 3.0 License.

Table 5. Previously analysed marine carbonate and seawater samples

Sample	Mineralogy	$\delta^{11}B$ range	Reference
Modern Coral	Aragonite	26.7-31.9	(Vengosh et al., 1991)
Modern Coral	Aragonite	23.0-24.7	(Hemming and Hanson, 1992)
Modern Coral	Aragonite	23.5-27.0	(Gaillardet and Allègre, 1995)
Modern Coral	Aragonite	23.9-26.2	(Hemming et al., 1998)
Modern Coral	Aragonite	25.2	(Allison and Finch, 2010)
Modern Coral	Aragonite	23.56-27.88	(Anagnostou et al., 2012)
Modern Coral	Aragonite	21.5-28.0	(Dishon et al., 2015)
Modern Coral	Aragonite	21.76-23.19	(Dissard et al., 2012)
Deep Sea Coral	Calcitic	13.7-17.3	(Farmer et al., 2015)
Modern Coral	Aragonite	18.52-23.96	(Holcomb et al., 2014)
Modern Coral	Aragonite	21.1-24.9	(Hönisch et al., 2004)
Modern Coral	Aragonite	23.2-28.7	(McCulloch et al., 2012)
Deep Sea Coral	Calcitic	15.5	(McCulloch et al., 2012)
Modern Coral	Aragonite	22.5-24.0	(Reynaud et al., 2004)
Modern Coral	Aragonite	31.1-35.7	(Rollion-Bard et al., 2011a)
Modern Coral	Aragonite	18.6-30.6	(Rollion-Bard et al., 2011b)
Modern Coral	Aragonite	21-24.5	(Schoepf et al., 2014)
Modern Coral	Aragonite	23.6-25.2	(D'Olivo et al., 2015)
Ancient Coral	Aragonite	23.6-27.1	(Douville et al., 2010)
Ancient Coral	Aragonite	24.5-27.1	(Kubota et al., 2014)
Ancient Coral	Aragonite	22.5-25.5	(Liu et al., 2009)
Modern Coral	Aragonite	21.1-25.4	(Wei et al., 2009)
Planktonic Foraminifera	Calcite	14.2-19.8	(Vengosh et al., 1991)
Planktonic Foraminifera	Calcite	22.0-23.3	(Sanyal et al., 1995)
Planktonic Foraminifera	Calcite	18.4	(Sanyal et al., 1997)
Benthic Foraminifera	Calcite	13.3, 20.3, 32.0	(Vengosh et al., 1991)
Benthic Foraminifera	Calcite	20.5, 21.4	(Sanyal et al., 1995)

Biogeosciences Discuss., doi:10.5194/bg-2017-154, 2017
Manuscript under review for journal Biogeosciences
Discussion started: 15 May 2017
© Author(s) 2017. CC-BY 3.0 License.

Biogeosciences
Discussions
Open Access
EGU

Bulk Foraminifera	Calcite	10.5, 11.5, 14.8, 16.2, 17.0	(Spivak et al., 1993)
Planktonic Foraminifera	Calcite	17.1, 22.9	(Kasemann et al., 2009)
Planktonic Foraminifera	Calcite	20.6-25.4	(Ni et al., 2007)
Benthic Foraminifera	Calcite	14.5 to 16.8	(Rae et al., 2011)
Benthic Foraminifera	Calcite	18-30.1	(Rollion-Bard and Erez, 2010)
Benthic Foraminifera	Calcite	15.8-17.4	(Yu et al., 2010)
Planktonic Foraminifera	Calcite	16.9-17.9	(Yu et al., 2013)
Planktonic Foraminifera	Calcite	19.1-22.2	(Bartoli et al., 2011)
Planktonic Foraminifera	Calcite	16.2-19.8	(Foster, 2008)
Planktonic Foraminifera	Calcite	15.2-17.2	(Foster et al., 2012)
Benthic Foraminifera	Calcite	13.09-13.37	(Foster et al., 2012))
Planktonic Foraminifera	Calcite	18.9-21.8	(Foster and Sexton, 2014)
Planktonic Foraminifera	Calcite	20.8-23.3	(Hönisch and Hemming, 2005)
Planktonic Foraminifera	Calcite	21.7-23.4	(Hönisch et al., 2009)
Benthic Foraminifera	Calcite	18.0	(Kaczmarek et al., 2015)
Planktonic Foraminifera	Calcite	15.1-16.4, 18.9-21.4	(Martínez-Botí et al., 2015a)
Planktonic Foraminifera	Calcite	19.1-19.8, 19.4-20.8	(Martínez-Botí et al., 2015b)
Planktonic Foraminifera	Calcite	24.2-25.7	(Palmer et al., 2010)
Mixed Foraminifera	Calcite	19.4-27.7	(Palmer, 1998)
Mixed Foraminifera	Calcite	20.8-26.6	(Pearson and Palmer, 1999)
Planktonic Foraminifera	Calcite	11-13.5*, 21.6-25.5	(Pearson and Palmer, 2000)
Benthic Foraminifera	Calcite	15.2-16.2	(Rae et al., 2014)
Planktonic Foraminifera	Calcite	13.6-15.8	(Penman and Hönisch, 2014)
Echinoid	High-Mg Calcite	22.7-22.9	(Hemming and Hanson, 1992)
Goniolithon	High-Mg Calcite	22.4	(Hemming and Hanson, 1992)
Encrusting Red Algae	High-Mg Calcite	23.0	(Hemming and Hanson, 1992)
Thecidellina	Calcite	21.5-22.5	(Hemming and Hanson, 1992)
Other Carbonates	Aragonite	19.1-24.8	(Hemming and Hanson, 1992)
Seawater	Seawater	39.9-40.2	(Hemming and Hanson, 1992)
Seawater	Seawater	37.7-40.4	(Foster et al., 2010)

Biogeosciences Discuss., doi:10.5194/bg-2017-154, 2017
Manuscript under review for journal Biogeosciences
Discussion started: 15 May 2017
© Author(s) 2017. CC-BY 3.0 License.

Figures

Fig. 1. (a) Speciation of dissolved inorganic boron ($B(OH)_3$ and $B(OH)_4^-$) as a function of seawater pH. (b) $\delta^{11}B$ of dissolved inorganic boron species as a function of seawater pH.

Fig. 2. Plot of literature-derived $\delta^{11}B$ for corals, foraminifera and brachiopods. The two gray lines indicate the theoretical seawater borate $\delta^{11}B$-pH curves that have been applied most frequently to interpret $\delta^{11}B$ variability in marine calcifiers. The pK_B is 8.6152 at 25 °C and 32 psu (Dickson, 1990).

Fig. 3. Elution curves indicating cumulative yield of boron for different volumes of the boron-specific resin (Amberlite IRA 743) placed in an ion exchange column.

Fig. 4. Boron isotopic composition (± SD) of different marine calcifying organisms with respect to seawater pH (± SD). The six species shown in this figure were grown under controlled pCO_2 conditions of *ca.* 409 ppm. Gray lines are theoretical seawater borate $\delta^{11}B$-pH curves based on different fractionation factors (α) that have been used to describe boron isotope fractionation between borate ion and boric acid in seawater (using pK_B of 8.6152 at 25°C and 32 psu). Although α = 1.0272 (Klochko et al., 2006) is the most commonly used α at present, borate $\delta^{11}B$-pH curves calculated from other values of α are also shown for reference.

Biogeosciences Discuss., doi:10.5194/bg-2017-154, 2017
Manuscript under review for journal Biogeosciences
Discussion started: 15 May 2017
© Author(s) 2017. CC-BY 3.0 License.

Author Contribution

RAE conceived of the project. RAE and JBR wrote the proposals that funded the work. JBR cultured the organisms. RAE, JNS, and JBR contributed to experimental design. JNS, Y-WL, MG, EP, and RAE contributed to method development. JNS performed the measurements with assistance from EP. JNS conducted the data analysis. Interpretation was led by JNS and RAE with input from JBR and Y-WL. JNS drafted the paper, which was edited by all authors.

Biogeosciences Discuss., doi:10.5194/bg-2017-154, 2017
Manuscript under review for journal Biogeosciences
Discussion started: 15 May 2017
© Author(s) 2017. CC-BY 3.0 License.

Acknowledgements

This work was supported by the "Laboratoire d'Excellence" LabexMER (ANR-10-LABX-19) and co-funded by a grant from the French government under the program "Investissements d'Avenir", and by a grant from the Regional Council of Brittany (SAD programme). RAE and JBR also acknowledge support from National Science Foundation grants OCE-1437166 and OCE-1437371. We thank J.-P. D'Olivo and the members of the UWA lab for supplying us with an aliquot of the NEP standard.

Biogeosciences Discuss., doi:10.5194/bg-2017-154, 2017
Manuscript under review for journal Biogeosciences
Discussion started: 15 May 2017
© Author(s) 2017. CC-BY 3.0 License.

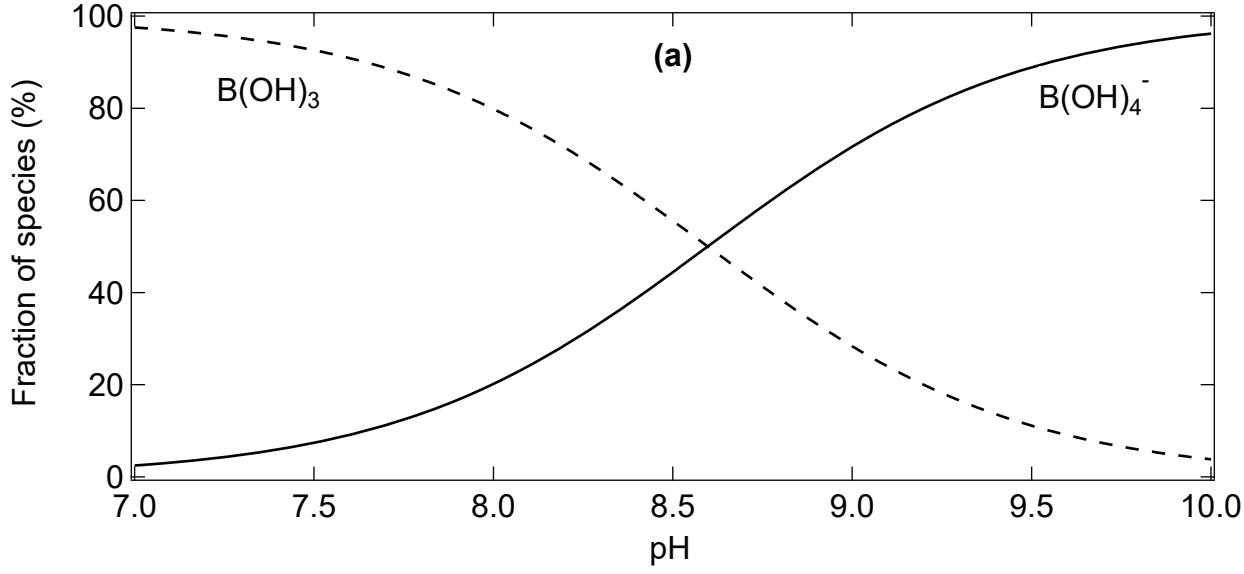

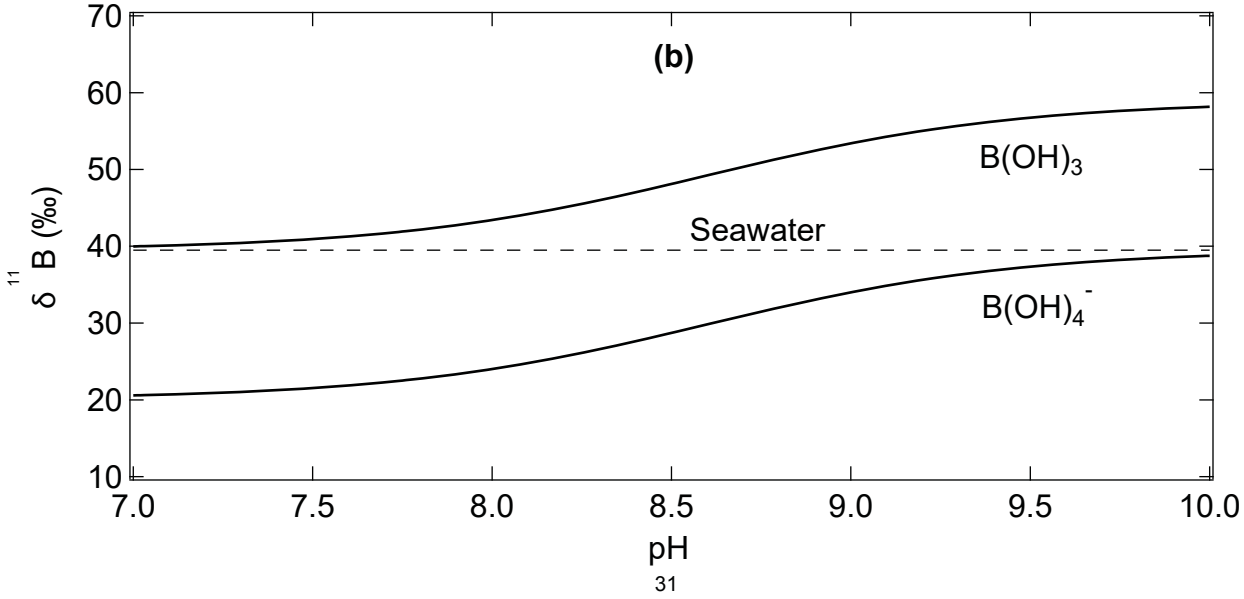

Biogeosciences Discuss., doi:10.5194/bg-2017-154, 2017
Manuscript under review for journal Biogeosciences
Discussion started: 15 May 2017
© Author(s) 2017. CC-BY 3.0 License.

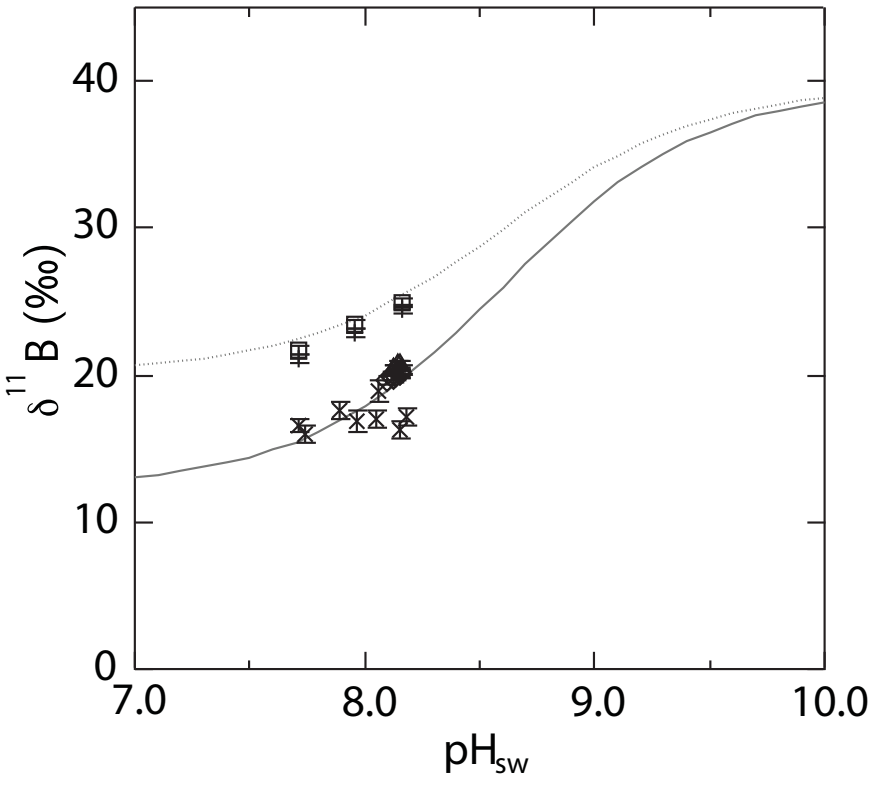

Seawater borate
α = 1.0272 (Klochko et al. 2006)
Seawater borate
α = 1.0194 (Kakihana et al. 1977)

\+ *Acropora nobilis* (Hönish et al. 2004)
□ *Porites cylindrica* (Hönish et al. 2004)
△ *G. ruber* (Foster, 2008)
◇ *G. sacculifer* (Foster, 2008)
× Brochiopod (Penmen et al. 2013)

Biogeosciences Discuss., doi:10.5194/bg-2017-154, 2017
Manuscript under review for journal Biogeosciences
Discussion started: 15 May 2017
© Author(s) 2017. CC-BY 3.0 License.

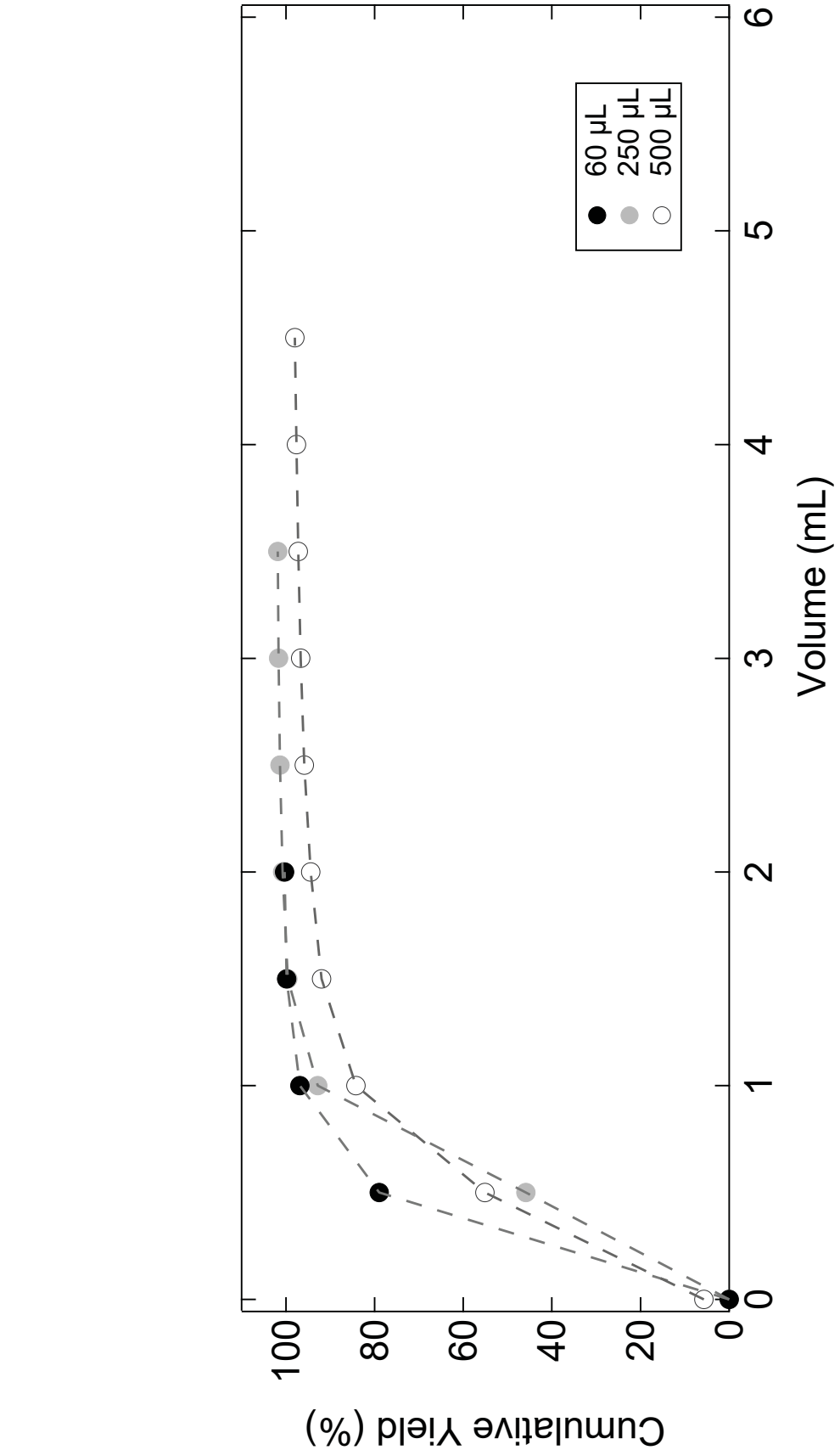

Biogeosciences Discuss., doi:10.5194/bg-2017-154, 2017
Manuscript under review for journal Biogeosciences
Discussion started: 15 May 2017
© Author(s) 2017. CC-BY 3.0 License.

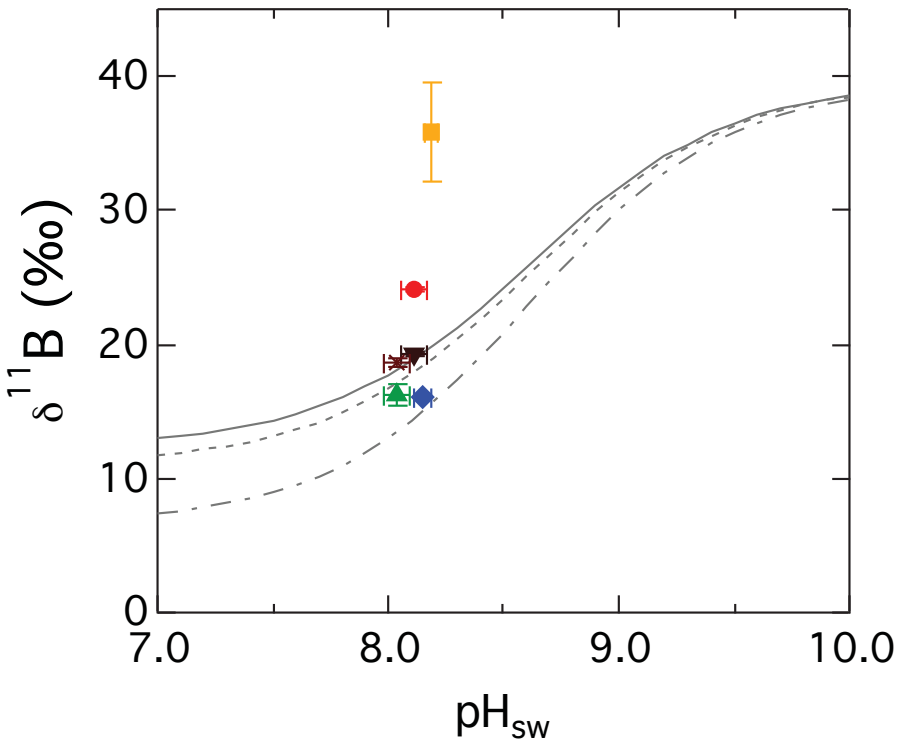

Seawater borate
α = 1.0272 (Klochko *et al.*, 2006)
Seawater borate
α = 1.0285 (Byrne *et al.*, 2006)
Seawater borate
α = 1.0330 (Palmer *et al.*, 1987)

Temperate coral
Coralline red alga
Temperate urchin
Serpulid
Tropical urchin
American oyster